CHAPTER 6

The effects of a small-scale flow fluctuation on hyporheic filtration processes

6.1 Introduction

Fluctuations in flow largely drive the exchange of water between the stream and hyporheic zone (Brunke and Gonser 1997), and govern biological processes by providing the nutrients, oxygen, and food required by the diverse biota of invertebrates and microorganisms (Findlay 1995). In regulated rivers, fluctuations in flow are controlled to suit human requirements, or as environmental flows to address perceived ecological needs. Until recently, little consideration has been given to the hyporheic zone in the release of environmental flows, and consequentially, the effects of environmental flows on hyporheic processes have not been studied (Boulton 2000b).

6.1.1 The importance of different sized flow fluctuations

The effect of flow on the hyporheic zone will be determined to a large extent by flow magnitude. For example, a large bed-moving flood will physically remove parts of the hyporheic zone and deposit them elsewhere, flushing nutrients, silt, and fauna from the sediment in the process. Following large floods, the recovery of some hyporheic elements (e.g. the invertebrate community) may take a long time. In the Danube River near Vienna, Austria, major flooding deposited sediments and re-initiated a cycle of bed clogging, while minor floods increased the hydraulic connection between the stream and groundwater (Blaschke *et al.* 2003). A moderate increase in flow will extend the hydrological boundaries of the hyporheic and parafluvial habitats, and flush water and silt from some of the sediments, as was observed in the Hunter River at BOWM and MOSE (Chapter 5). Large to moderate flow fluctuations still occur in regulated rivers, though often at a reduced frequency and magnitude to natural conditions. However, small fluctuations (up to 10 cm increase in river stage) are most frequent in natural rivers and may be at least as important to near-stream parafluvial and hyporheic processes as less frequent larger flows.

6.1.2 Small-scale fluctuations

The prevention of pumping for the first 12 h of a large flow event as specified by Flow Rule 2 effectively provides a medium to large flow (discussed in Chapter 5),

complemented by a small-scale flow (Figure 6.1). During the initial 12 h of high flow, the ban on pumping allows water levels to increase. After this, water-level may start to decline naturally, or due to the commencement of pumping. This effectively creates a small-scale flood pulse at the higher margins of the bar, where sediments are temporarily submerged for approximately half a day (Figure 6.1).

Small pulses on their own are unlikely to significantly affect the geomorphological characteristics of a river. However, the re-wetting of sediments may have important consequences for shallow parafluvial and hyporheic biological activity through slight increases in hydraulic exchange and saturation of previously dry sediments. As river stage rises, it is predicted that there will be an increase in oxygen-rich water entering the sediments of the bar and bed. This will increase the activity of the aerobic microbiota, alter the redox environment, and thus enhance the biological and chemical filtration of the water. It is not certain how long this microbial activity will persist when surface flow declines but key ecosystem processes, such as the removal of soluble phosphorus, occur during drying which influence the nutrient dynamics of the river.

Studies from lake sediments indicate that reflooding sediments leads to an initial release of phosphorus from the sediments (Qiu and McComb 1995, Figure 6.2). In lotic environments, phosphorus that is released from the sediments in the slow-flowing hyporheic zone, then into the overlying water, will be removed rapidly downstream. As the water level subsides and sediments dry, bacteria are able to remove soluble phosphorus from water and incorporate it into the particulate phase (Qiu and McComb 1995). This is also the case for abiotic retention of phosphorus, where aerobic conditions lead to the oxidation of phosphorus with ferric, aluminium, or manganese hydroxides, and sorption to clay and calcium compounds (Hendricks and White 2000). In this way, the sediments store phosphorus until the next time the sediments are inundated and are able to release it downstream (Figure 6.2).

In the case of nitrogen, McComb and Qiu (1998) suggest that as sediments dry, enhanced mineralisation of organic matter contributes to an increase of ammonium. Ammonium is the most labile form of nitrogen, but it is often in low concentrations in streams, being dominated by higher concentrations of nitrates (Webster *et al.* 2003). Re-wetting of the sediments liberates ammonium into the overlying water. In standing

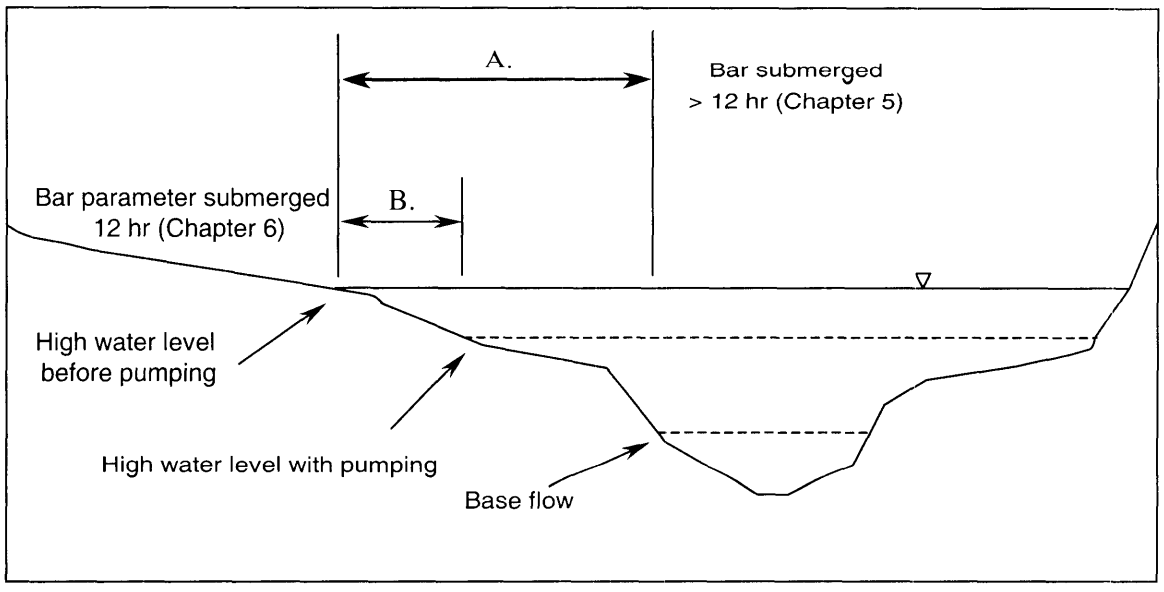

Figure 6.1. Pictorial representation of the dual flow events brought about by Flow Rule 2. Initially, water level rises with the commencement of high flow (A). After 12 hours, pumping is allowed, and water level declines (B). The holistic effects of Flow Rule 2 were examined in Chapter 5.

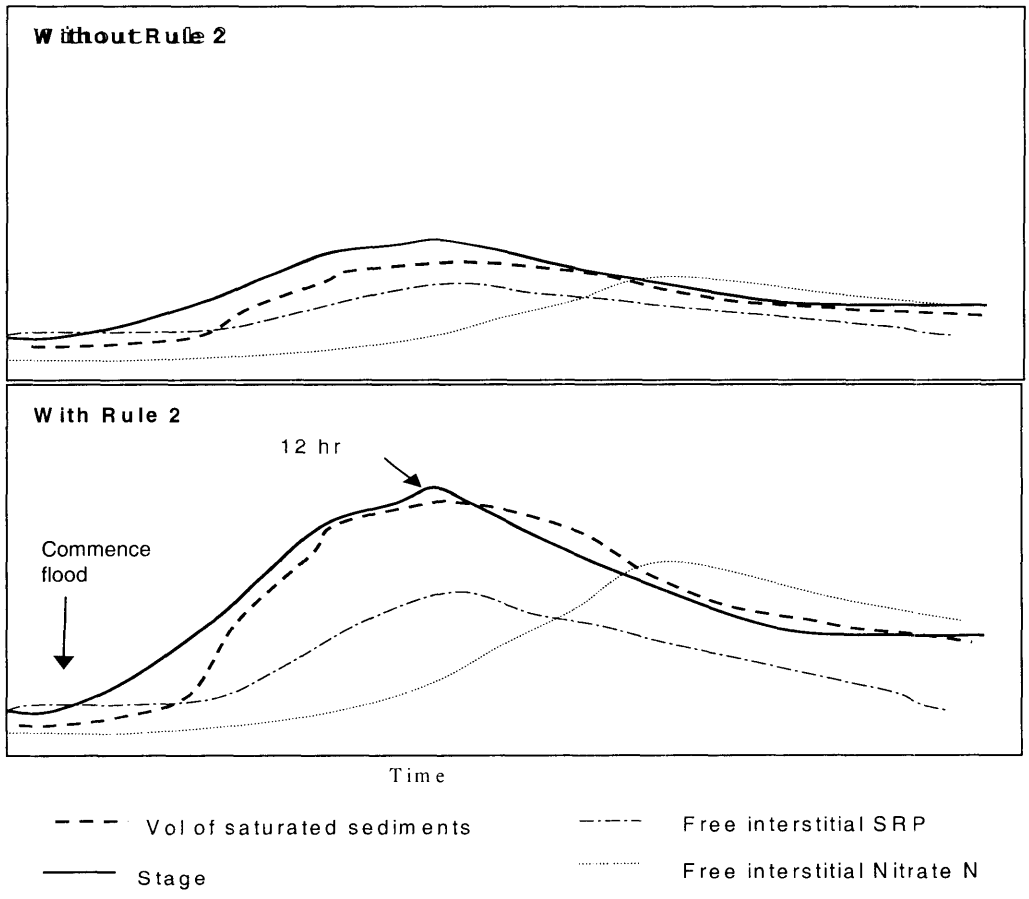

Figure 6.2. Without Rule 2, pumping prevents the maximum stage of the river from being achieved and less of the hyporheic filters become saturated. The ban on pumping for the first 12 hours allows river levels to rise and a larger volume of sediments to become saturated.

waters, this enhances nitrification in the waters above the sediment, and potentially leads to nitrogen removal from the water as plants absorb nitrates. In the lotic waters that overlie recently inundated parafluvial bars, it is likely that the ammonium will be rapidly swept downstream, and that stimulation of nitrifying bacteria will not occur in the surface waters. However, within the sediment interstices the hyporheic water is likely to remain long enough for there to be significant nitrification (Figure 6.2). As this water enters the surface water, or comes into contact with roots it is absorbed by plants and algae. This will be especially evident at the highly oxygenated wetted interstitial interface as ammonium N-rich parafluvial water levels rise with the increase in river stage.

6.1.3 A conceptual model

The potential effects of small scale flow fluctuations, both natural and those resulting from Flow Rule 2, can be tested against predictions from a conceptual model. At low flows, where hyporheic exchange is reduced and there is a dominance of anaerobic conditions, the hyporheic and parafluvial zones serve as transient storages areas for ammonium (Duff and Triska 2000). As water in the Hunter River rises, so too does the interstitial water in adjacent bars. This raises the interstitial boundary between saturated and unsaturated sediments and makes a larger volume of sediment available to the parafluvial processes, such as nitrification in the 'oxygenated fringe' (Lamontagne *et al.* 2003). Therefore, it is expected that the initial re-wetting of the sediments will stimulate a release of phosphorus (Qiu and McComb 1995). The influx of oxygenated stream water will subsequently stimulate nitrification in the ammonium-rich sediments, increasing the concentration of nitrate in the hyporheic zone (Duff and Triska 2000). Coupled with this is the increased rate with which water moves through the sediment. Although still slow compared to the stream water, it will constantly move the nutrients along flowpaths in the bar and eventually into the stream where it will rapidly be removed.

In accordance with Flow Rule 2, pumping on the river commences 12 h later, lowering the water level and exposing the bar margins. Within the bars there is potentially a large increase of oxygenated water, due to diffusion at the air interface with the films of water coating sediment particles. Initially, while the sediments remain moist, this will lead to an increase in the concentrations of nitrate and SRP. However, as the upper sediments dry, bacterially aided adsorption will remove soluble phosphorus from the

water (Qiu and McComb 1995, Hendicks and White 2000). In the deeper, permanently wetted sediments, there will be an increase in ammonium due to denitrification and mineralisation in the sediments (Duff and Triska 2000). In effect, the bars will act as temporary nutrient sinks for nitrogen and phosphorus until a pulse once again inundates them and the nutrients are washed downstream.

Faunal communities are also predicted to change in response to these small fluctuations in water level. The weak hydraulic pressure exerted by these flows probably means that any changes in faunal communities occur through active migration rather than the invertebrates being passively pushed by the water. As water level in the bar increases, groundwater fauna may move upward to take advantage of the newly created area of habitat. Epigean taxa might also take advantage of the newly created feeding grounds. When water recedes, the once-submerged sediments will harbour small surface-dwelling invertebrates that were stranded, and had little choice but to move down. However, many of these will die as aerobic conditions decline. To test the validity of this model at two sites in the Hunter River, a series of physico-chemical, nutrient, microbial, and faunal variables was measured before, during, and following a small increase in water level using a flow diversion.

6.2 Study sites

Moses Crossing (MOSE) and Bowmans Crossing (BOWM) were the two sites selected for this study. These sites were selected because they had low areas of bar close to the river, over which water could be easily channelled with a small diversion. Further descriptions of these sites are given in Chapters 2, 3 and 5.

6.3 Methods

6.3.1 Field sampling

Sampling commenced at Bowmans Crossing (BOWM) on 19 March 2002, and at Moses Crossing (MOSE) on 25 March 2002. At each site samples were collected at 12 h (1900 h), and 0 h (0700 h) prior to the construction of a flow deflection fence (Figure 6.3). Inundation samples were collected at 2 h (0930 h) and 12 h (1930 h) while water was deflected over the bar. Following the collection of the 12 h samples, the deflection fence was removed. Post-inundation samples were collected at 24 h (0730 h, 12 h following the removal of the fence and 33 h (1630 h).

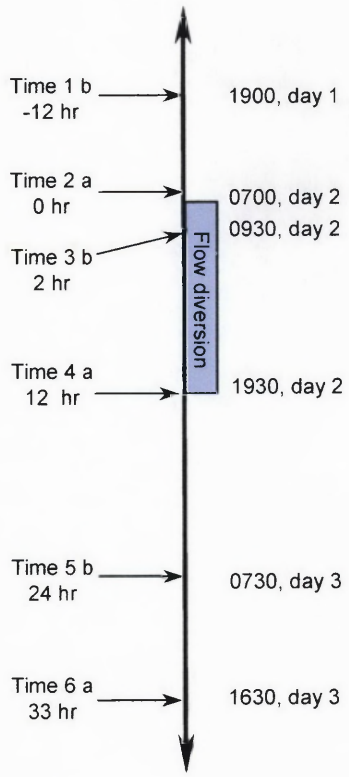

Figure 6.3. Timeline showing the seven sampling occasions. a indicates that all variables were collected (nutrients, fauna, physico-chemical, and FDA), b indicates that only some variables were collected (nutrients without ammonium, and physico-chemical).

Figure 6.4. Looking downstream at Moses Crossing with the flow deflection fence in place.

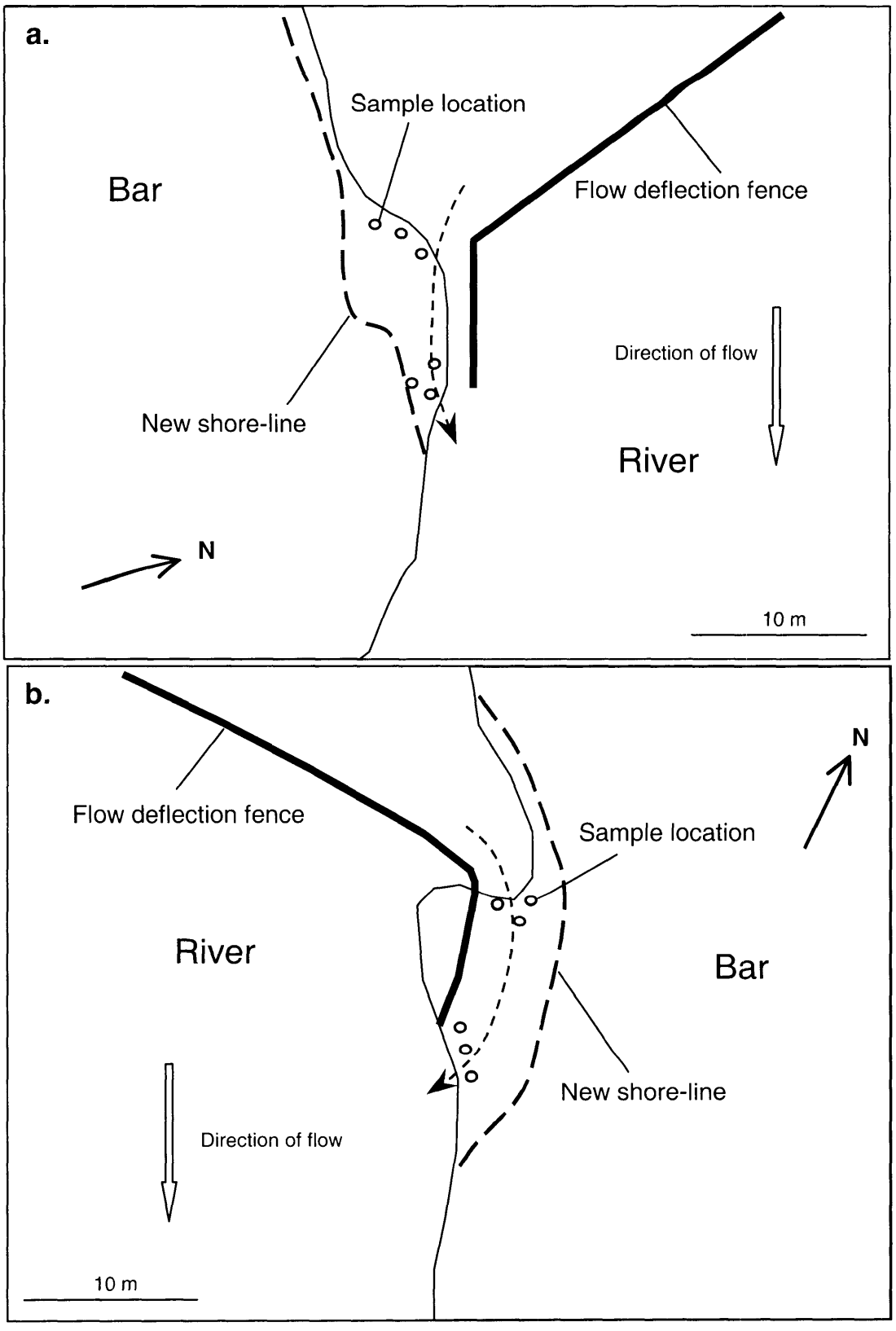

Figure 6.5. The location of the flow deflection fence at (a) Bowmans Crossing, and (b) Moses Crossing.

Water was diverted over the bar with a flow-deflection fence consisting of 5-cm meshed wire overlain with plastic sheeting and supported by metal fence-posts (Figure 6.4). At BOWM water was diverted, with a 23 m fence, over a previously dry margin of the leading edge of bar on the right side of the river (Figure 6.5a). During the diversion, water depth over the bar was between 45 and 130 mm. Flow diversion at MOSE was over a small peninsula that protruded into the river (Figure 6.5b). Here, the fence was 30 m long, and water flowing over the bar was 25 to 140 mm deep.

Triplicate samples were collected from the leading edge of bar, and from a point along the bar at the probable end of the parafluvial flowpath (Figure 6.5). At both sites the 'tail bar' location was 10 m downstream of the 'head bar'. Each location was sampled from 13 mm internal diameter PVC piezometers sunk to 10 and 30 cm below the consolidated sediment. These were left in situ for the duration of sampling. For each of the six times, water samples were collected with a 60 mL syringe and 3 mm diameter rubber tubing. After discarding the initial 50 mL, 125 mL was filtered through Whatman GF/C filter papers into a pre-rinsed acid washed polyurethane bottle, and frozen until analysis for nitrate/nitrite (NOx) and soluble reactive phosphorus (SRP). A further 125 mL was extracted and placed in a separate bottle without filtering. This was later analysed for total phosphorus (TP) and total nitrogen (TN). As well, dissolved oxygen (DO), temperature, electrical conductivity (EC), and pH were measured with a YSI model 57 DO meter with a YSI5739 probe (Yellow Springs Instruments, Ohio) and a TPS MC81 pH/conductivity meter (TPS instruments, Brisbane, Queensland). Duplicate surface samples were collected for each variable from the main channel, < 10 m upstream from the 'head' habitat. Hydraulic head was measured at each minipiezometer using the probe described in section 5.3.2. In Chapter 5, hydraulic head was measured from only one depth, therefore there was no difference in pressure exerted on the water between samples. However, since samples in the current chapter were recorded from two depths, the increase in hydraulic pressure due to the different depths had to be considered and hydraulic head was converted to vertical hydraulic gradient (VHG). VHG was calculated by dividing the hydraulic head in centimetres by sampling depth in centimetres (Pepin and Hauer 2002).

At one time before (Time 2), during (Time 4), and after (Time 6) the flow diversion, a sample of 24 mL was taken from each mini piezometer for ammonium analysis. This was fixed with 1 mL of phenol and cooled to between 0 and 4 °C until analysis (within 3 days of collection). Additional 6 L samples were collected following the initial physico-chemical samples. These were elutriated through a 125 μm sieve to remove fauna, and sediments less than 125 μm were left to settle before being removed to zip-seal bags and, within 2 h, analysed for microbial hydrolytic activity (see later). Fauna samples were stained with Rose Bengal and stored in 100 % ethanol until processing.

Bacterial hydrolytic activity was analysed using a modified version of the method described by Battin (1997). Within 2 h of collection, approximately 6 mL of the fine sediment (< 125 μm) slurry was transferred to a pre-weighed acid-washed jar. This sediment was then weighed, and added to 3 mL of KH_2PO_4 / Na_2HPO_4 buffer (pH = 7.6). Incubation with 0.1 mL of FDA solution (20 mg fluorescein diacetate, Sigma Chemicals, St Louis, USA, dissolved in 6 mL acetone and 4 mL filtered distilled water) was timed until a faint green tinge of fluorescein was detected. The reaction was then stopped with 3 mL of acetone and the solution snap frozen to prevent further activity.

6.3.2 Laboratory analysis

Ammonium samples were analysed using the phenol-hypochlorite method (Soloranzo 1969). NOx concentration was determined with the cadmium reduction method (Wood *et al.* 1967), and SRP with the molybdate blue method (Murphy and Riley 1962). TN and TP were analysed using persulphate digestion (Hosomi and Sudo 1986).

FDA samples were thawed and centrifuged to separate sediment from the liquid. Fluorescein concentration was determined by measuring the absorbance of the supernatant. The rate of hydrolysis of FDA, in μmole g^{-1} hr^{-1}, was then calculated with

$$\frac{(OD / 81.3) * (DF + w)}{(m*t)}$$

where OD is the measured optical density, 81.3 is the absorption coefficient for FDA, DF represents the dilution factor, w is the interstitial water volume (mL), m is the mass of dry sediments (g), and t is the incubation time in hours.

Faunal samples were sorted under 10 – 400 x magnification and identified as far as possible. Some taxa (e.g. oligochaete worms, microturbellarian flatworms, cyclopoid copepods) were grouped because they appeared to be functionally equivalent.

6.3.3 Statistical analysis

Repeated measure analysis of variance (ANOVA) tests were used to detect significant differences between flow treatments in the mean concentrations of interstitial NOx-N, total N, SRP, total P, dissolved oxygen, temperature, pH, electrical conductivity, and hydraulic head. Separate analyses were done for each site with Treatment, Time nested in Treatment, Habitat, and Depth being the four factors. Treatment, Habitat, and Depth were treated as fixed, while Time nested in Treatment was treated as random. For these analyses, Treatment had three levels, (Before, During, and After the release), Time nested in Treatment had two levels, Habitat had two levels (Head and Tail), and Depth had two levels (10 cm and 30 cm).

Three-factor crossed analysis of variance was used to test for differences in the means of interstitial NH_4, FDA, invertebrate abundance (I), and taxonomic diversity (Tx). This was because only one set of samples were collected for each treatment, removing the need to nest Time in Treatment. The three fixed factors for this were Treatment, Habitat, and Depth, with all of these having the same number of levels as their corresponding factors in the analysis mentioned above.

For those variables measured from the surface water (NOx-N, total N, SRP, total P, dissolved oxygen, temperature, pH, electrical conductivity), two-factor mixed ANOVAs were used to test for differences in the means. The factors here were Treatment (fixed, with three levels), and Time nested within treatment (random, with two levels).

Prior to analysis all data were tested for normality using Wilk-Shapiro tests in Statistix version 7 (Analytical Software 2000). Where necessary, appropriate transformations were carried out. Box plots and plots of residuals were examined after analysis, and where variances were not homogenous analysis was re-done with transformed data. For all ANOVAs, Tukey's pairwise tests were conducted *post hoc* and analyses were done using SYSTAT for Windows, version 9.0 (SYSTAT Incorporated, Evanston, Illinois, USA).

At each site, temporal differences in invertebrate communities were assessed using non-metric multidimensional scaling (nMDS). The significance of groupings was determined with 10 000 permutations of analysis of similarities (ANOSIM). Two separate ANOSIMs were done for each site. The first crossed Time with Habitat whereas the second crossed Time with Depth. Bray-Curtis similarity matrices on log (x+1) transformed data were used for MDS and ANOSIM analysis. Similarity percentages (SIMPER) were used to determine the major taxa contributing to each factor grouping. Data were log (x+1) transformed for SIMPER analysis.

6.4 Results

6.4.1 Vertical hydraulic gradient (VHG)

VHG at both sites was more negative at the head of the bar than it was positive at the tail ($P < 0.001$ at BOWM, $P = 0.003$ at MOSE, Table 6.1, Figure 6.6). At BOWM, the flow deflection increased upwelling in the tail ($P = 0.011$, Table 6.1, Figure 6.6), but downwelling was not significantly increased. VHG at MOSE increased in both head and tail habitats when water was diverted over the bar ($P = 0.023$, Table 6.1, Figure 6.6). At both sites the VHG returned to pre-diversion levels once the deflection fence was removed.

6.4.2 Physico-chemical variables

DO saturation in the stream at BOWM varied from 72.45 ± 0.97 to 125.40 ± 0.97 % saturation during this study (Figure 6.7) but did not change significantly with Treatment ($F_{2,6} = 0.195$, $P = 0.832$). When the water was channelled over the bar, DO in both interstitial habitats at 10 cm increased significantly, but at 30 cm, only DO in the tail increased ($P = 0.028$, Figure 6.7, Table 6.2). Following the removal of the fence, the DO of interstitial water remained high in both habitats.

DO fluctuated over a similar range in the stream at MOSE as it did at BOWM (79.28 ± 0.01 and 130.95 ± 2.24 % saturation, Figure 6.7). Surface DO at MOSE changed with each treatment, being highest during the diversion ($F_{2,6} = 28.80$, $P = 0.011$, Figure 6.7). In the subsurface, DO increased while water was being deflected over the bar ($P = 0.031$, Table 6.2, Figure 6.7). Following the removal of the fence, DO in the tail fell to pre-deflection concentrations, while DO at the head of the bar remained at concentrations comparable to those during the diversion. DO was always higher at the

head of the bar than the tail (P = 0.040, Table 6.2), and saturations declined with depth (P = 0.009, Table 6.2).

Stream temperature fluctuated diely within treatments at BOWM ($F_{3,6}$ = 1188.515, P < 0.001, Figure 6.8). Temperature in the morning (22.6 ± 0.5 to 25.5 ± 1.0 °C, Figure 6.8) was lower than in the evening (28.0 ± 0.0 to 28.8 ± 0.2 °C). Interstitial temperature fluctuated similarly, displaying diel patterns rather than flow-determined patterns (P < 0.001, Table 6.3, Figure 6.8).

The mean surface water temperature at MOSE ranged between 21.8 ± 0.1 and 25.4 ± 0.1 °C and was highest during the flow diversion ($F_{3,6}$ = 16.00, P = 0.025). Interstitial temperatures ranged between 18.7 ± 0.2 °C and 25.8 ± 0.6 °C and also appeared to be affected by diel patterns rather than the flow manipulation (P < 0.001, Table 6.2, Figure 6.8).

Conductivity in BOWM surface water ranged between 0.65 ± 0.04 and 0.76 ± 0.01 mS/cm but did not vary significantly throughout the study ($F_{2,6}$ = 2.8, P = 0.102). Interstitial EC changed with time within each treatment (P < 0.001, Table 6.4, Figure 6.9) but not among treatments (P = 0.448, Table 6.4, Figure 6.9).

At MOSE, EC in the surface water did not vary significantly ($F_{2,6}$ > 50, P > 0.999), remaining between 0.62 ± 0.01 and 0.67 ± 0.01 mS The mean interstitial EC decreased during the flow diversion at the tail of the bar but not at the head (P = 0.019, Table 6.4, Figure 6.9). EC also varied between the two times within each treatment (P < 0.001, Table 6.4, Figure 6.9). At all times before and after the release, conductivity at the tail of the bar exceeded 0.7 mS/cm (Figure 6.9), and this habitat had ECs that typically exceeded downwelling EC (P = 0.002, Table 6.4, Figure 6.9).

The pH of BOWM surface water was between 7.75 ± 0.00 and 8.76 ± 0.10. Surface pH varied within each treatment ($F_{3,6}$ = 26.93, P = 0.001) but was not different among treatments (Figure 6.10). Within each treatment, interstitial pH was lower for the second time than the first (P < 0.001, Table 6.5, Figure 6.10). Interstitial pH was not affected by the flow diversion.

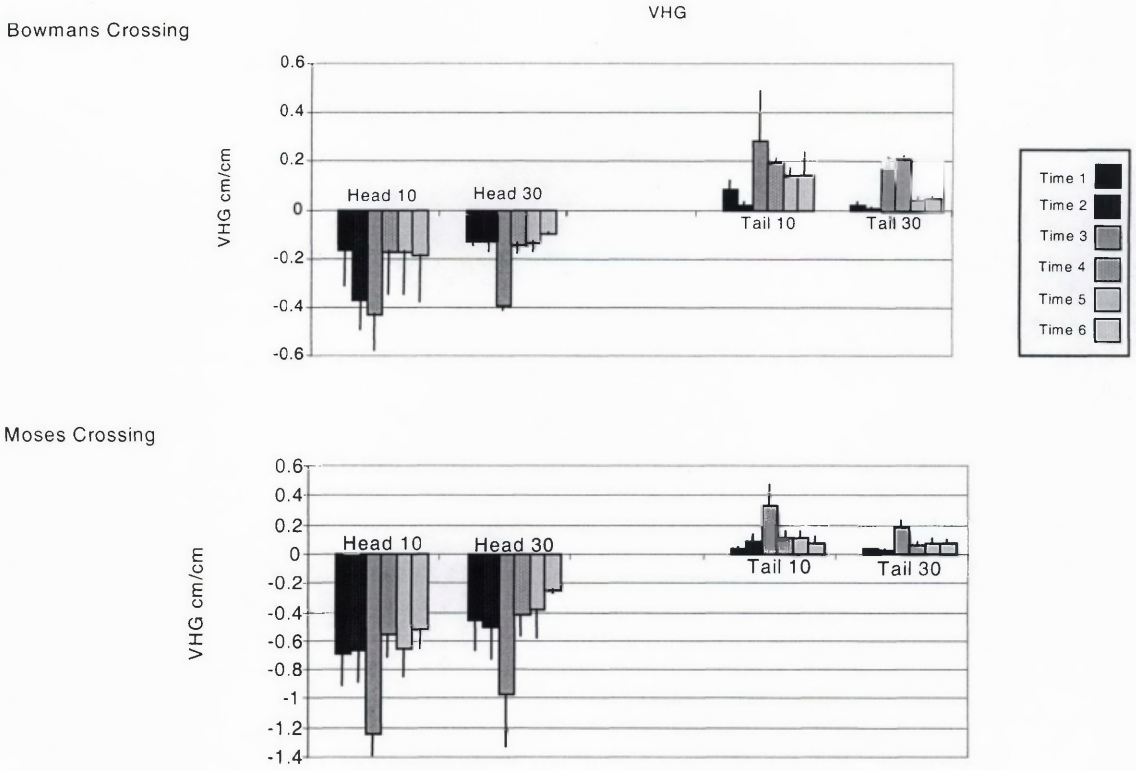

Figure 6.6. Mean (+ or - SE) VHG at Bowmans Crossing and Moses Crossing over the six times of the survey.

Table 6.1. ANOVA results table for VHG for the main factors and interaction terms. Bold figures are significant at P = 0.05. Tr = Treatment, H = Habitat, D = Depth, T(Tr) = Time nested in Treatment.

Source	SS	df	MS	F-ratio	P
Bowmans Crossing - rank transformed					
Tr	1471.000	2	735.500	5.113	0.108
H	21736.125	1	21736.125	1318.451	**0.000**
D	636.056	1	636.056	8.844	0.059
Tr*H	950.250	2	475.125	28.820	**0.011**
Tr*D	105.194	2	52.597	0.731	0.551
H*D	39.014	1	39.014	0.394	0.533
Tr*D*H	367.694	2	183.847	5.635	0.096
T(Tr)	431.583	3	143.861	1.452	0.239
H*T(Tr)	49.458	3	16.486	0.166	0.919
D*T(Tr)	215.750	3	71.917	0.726	0.542
H*D*T(Tr)	97.875	3	32.625	0.329	0.804
Error	4756.000	48	99.083		
Moses Crossing - rank transformed					
Tr	563.271	2	281.635	16.933	**0.023**
H	23328.000	1	23328.000	79.934	**0.003**
D	33.347	1	33.347	1.194	0.354
Tr*H	884.896	2	442.448	1.516	0.351
Tr*D	129.799	2	64.899	2.324	0.246
H*D	572.347	1	572.347	6.058	**0.017**
Tr*D*H	8.757	2	4.378	1.046	0.452
T(Tr)	49.896	3	16.632	0.176	0.912
H*T(Tr)	875.521	3	291.840	3.089	**0.036**
D*T(Tr)	83.771	3	27.924	0.296	0.828
H*D*T(Tr)	12.563	3	4.188	0.044	0.987
Error	4534.833	48	94.476		

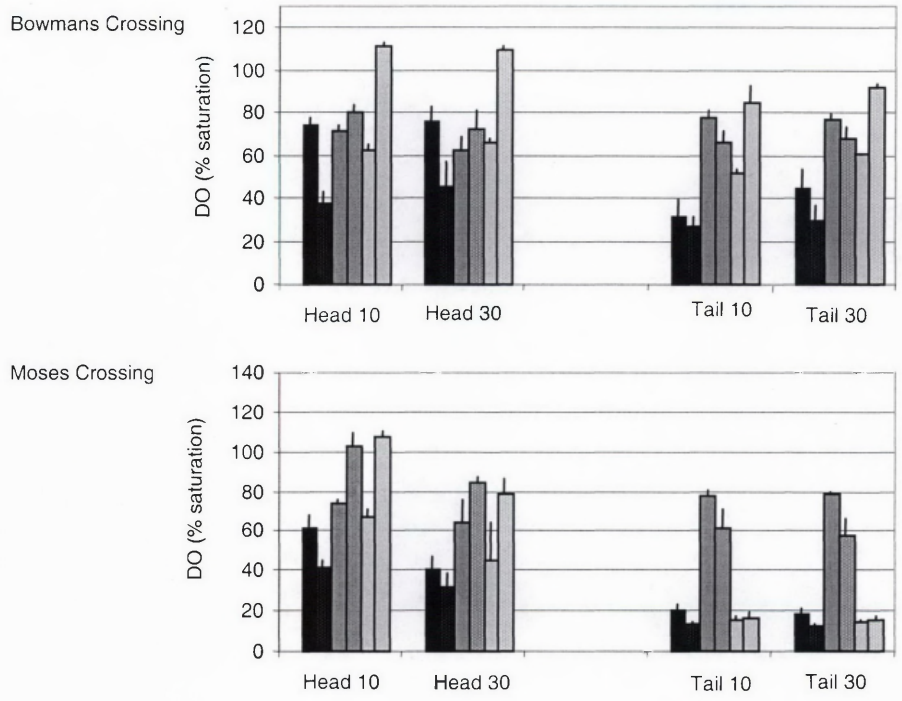

Surface DO (mg/L)	Time 1	Time 2	Time 3	Time 4	Time 5	Time 6
Bowmans Crossing	97.70 ± 1.04	72.45 ± 0.97	87.25 ± 6.62	105.03 ± 0.53	72.95 ± 0.39	125.40 ± 0.97
Moses Crossing	100.48 ± 0.00	79.28 ± 0.00	80.41 ± 0.00	130.95 ± 2.24	81.16 ± 0.35	111.05 ± 0.48

Figure 6.7. Mean (+ SE) dissolved oxygen (DO) at Bowmans Crossing and Moses Crossing over the six times of the survey. Table beneath graphs indicates mean (± SE) surface values.

Table 6.2. ANOVA results table for dissolved oxygen for the main factors and interaction terms. Bold figures are significant at P = 0.05. Tr = Treatment, H = Habitat, D = Depth, T(Tr) = Time nested in Treatment.

Source	SS	df	MS	F-ratio	P
Bowmans Crossing					
Tr	15493.754	2	7746.877	1.929	0.289
H	3207.969	1	3207.969	5.664	0.098
D	91.028	1	91.028	7.717	0.069
Tr*H	1962.229	2	981.115	1.732	0.316
Tr*D	346.049	2	173.024	14.669	**0.028**
H*D	184.861	1	184.861	2.130	0.151
Tr*D*H	27.572	2	13.786	0.395	0.704
T(Tr)	12046.312	3	4015.437	46.272	**0.000**
H*T(Tr)	1699.079	3	566.360	6.526	**0.001**
D*T(Tr)	35.386	3	11.795	0.136	0.938
H*D*T(Tr)	104.819	3	34.940	0.403	0.752
Error	4165.366	48	86.778		
Moses Crossing					
Tr	25280.280	2	12640.140	13.707	**0.031**
H	19575.966	1	19575.966	12.115	**0.040**
D	1681.170	1	1681.170	35.529	**0.009**
Tr*H	6698.512	2	3349.256	2.073	0.272
Tr*D	106.351	2	53.175	1.124	0.432
H*D	1312.582	1	1312.582	14.117	**0.000**
Tr*D*H	139.654	2	69.827	2.722	0.212
T(Tr)	2766.480	3	922.160	9.918	**0.000**
H*T(Tr)	4847.375	3	1615.792	17.378	**0.000**
D*T(Tr)	141.954	3	47.318	0.509	0.678
H*D*T(Tr)	76.947	3	25.649	0.276	0.843
Error	4463.046	48	92.980		

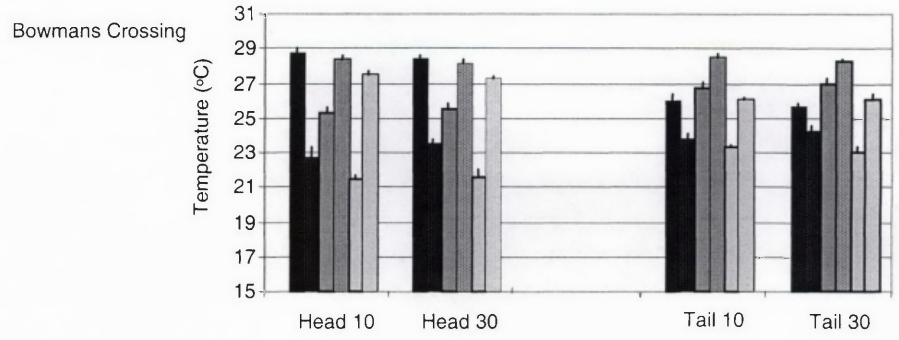

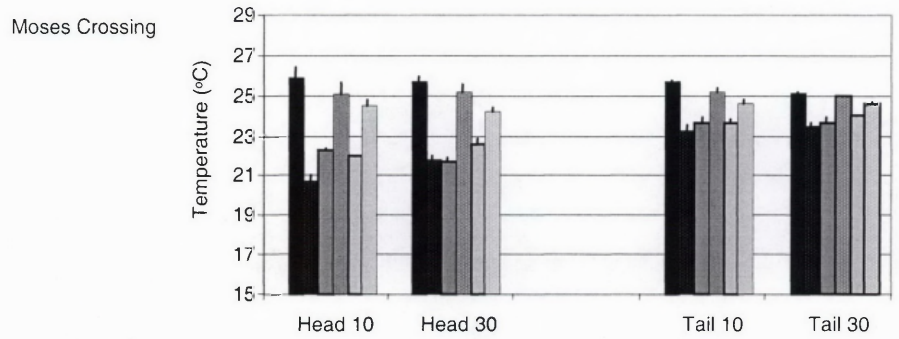

Surface Temp (°C)	Time 1	Time 2	Time 3	Time 4	Time 5	Time 6
Bowmans Crossing	28.0 ± 0.0	23.9 ± 0.1	25.5 ± 1.0	28.8 ± 0.2	22.6 ± 0.5	27.4 ± 0.1
Moses Crossing	25.2 ± 0.0	21.8 ± 0.0	22.0 ± 0.0	25.4 ± 0.1	22.8 ± 0.0	24.0 ± 0.0

Figure 6.8. Mean (+ SE) temperature at Bowmans Crossing and Moses Crossing over the six times of the survey. Table beneath graphs indicates mean (± SE) surface values.

Table 6.3. ANOVA results table for temperature for the main factors and interaction terms. Bold figures are significant at P = 0.05. Tr = Treatment, H = Habitat, D = Depth, T(Tr) = Time nested in Treatment.

Source	SS	df	MS	F-ratio	P
Bowmans Crossing					
Tr	91.187	2	45.594	0.608	0.600
H	0.002	1	0.002	0.000	0.991
D	0.000	1	0.000	0.000	0.995
Tr*H	8.654	2	4.327	0.373	0.717
Tr*D	0.120	2	0.060	0.096	0.911
H*D	0.064	1	0.064	0.243	0.624
Tr*D*H	0.019	2	0.009	0.131	0.882
T(Tr)	224.843	3	74.948	283.490	**0.000**
H*T(Tr)	34.837	3	11.612	43.924	**0.000**
D*T(Tr)	1.878	3	0.626	2.368	0.082
H*D*T(Tr)	0.213	3	0.071	0.268	0.848
Error	12.690	48	0.264		
Moses Crossing					
Tr	0.462	2	0.231	0.007	0.994
H	12.458	1	12.458	2.382	0.220
D	0.022	2	0.022	0.031	0.872
Tr*H	0.069	2	0.035	0.007	0.993
Tr*D	0.313	2	0.157	0.223	0.812
H*D	0.113	1	0.113	0.604	0.441
Tr*D*H	0.459	2	0.229	1.372	0.377
T(Tr)	106.347	3	35.449	189.658	**0.000**
H*T(Tr)	15.691	3	5.230	27.983	**0.000**
D*T(Tr)	2.107	3	0.702	3.757	**0.017**
H*D*T(Tr)	0.502	3	0.167	0.895	0.451
Error	8.972	48	0.187		

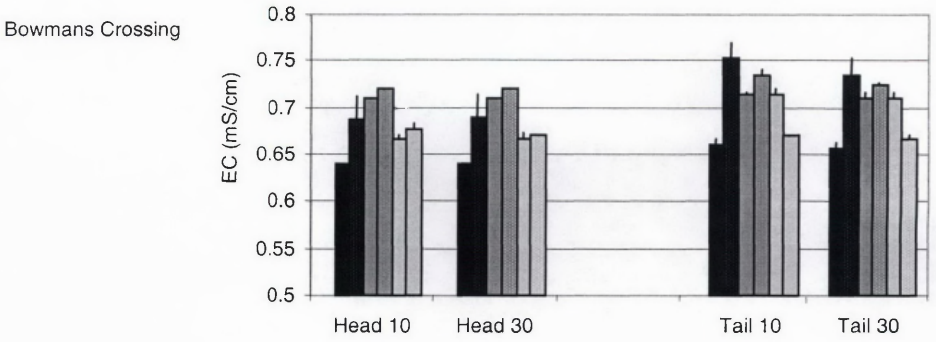

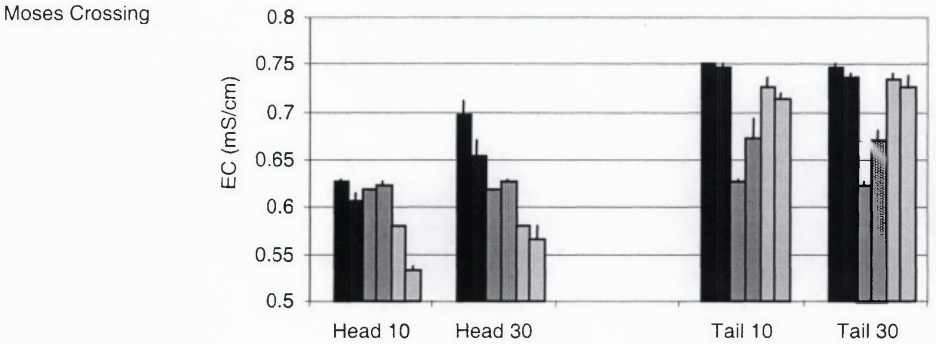

Surface EC (mS/cm)	Time 1	Time 2	Time 3	Time 4	Time 5	Time 6
Bowmans Crossing	0.66 ± 0.00	0.65 ± 0.04	0.76 ± 0.00	0.74 ± 0.04	0.74 ± 0.00	0.71 ± 0.00
Moses Crossing	0.67 ± 0.00	0.66 ± 0.00	0.66 ± 0.00	0.67 ± 0.00	0.64 ± 0.00	0.62 ± 0.00

Figure 6.9. Mean (+ SE) electrical conductivity at Bowmans Crossing and Moses Crossing over the six times of the survey. Table beneath graphs indicates mean (± SE) surface values.

Table 6.4. ANOVA results table for electrical conductivity for the main factors and interaction terms. Bold figures are significant at P = 0.05. Tr = Treatment, H = Habitat, D = Depth, T(Tr) = Time nested in Treatment.

Source	SS	df	MS	F-ratio	P
Bowmans Crossing					
Tr	0.021	2	0.011	1.064	0.448
H	0.008	1	0.008	3.911	0.142
D	0.000	1	0.000	8.167	0.065
Tr*H	0.003	2	0.002	0.774	0.536
Tr*D	0.000	2	0.000	0.167	0.854
H*D	0.000	1	0.000	0.774	0.383
Tr*D*H	0.000	2	0.000	1.091	0.441
T(Tr)	0.030	3	0.010	38.387	**0.000**
H*T(Tr)	0.006	3	0.002	7.527	**0.000**
D*T(Tr)	0.000	3	0.000	0.129	0.942
H*D*T(Tr)	0.000	3	0.000	0.237	0.870
Error	0.012	48	0.000		
Moses Crossing					
Tr	0.050	2	0.025	8.690	0.056
H	0.162	1	0.162	117.670	**0.002**
D	0.003	1	0.003	9.363	0.055
Tr*H	0.054	2	0.027	19.615	**0.019**
Tr*D	0.002	2	0.001	3.403	0.169
H*D	0.003	1	0.003	13.308	**0.001**
Tr*D*H	0.004	2	0.002	14.011	**0.030**
T(Tr)	0.009	3	0.003	12.994	**0.000**
H*T(Tr)	0.004	3	0.001	6.252	**0.001**
D*T(Tr)	0.001	3	0.000	1.421	0.248
H*D*T(Tr)	0.000	3	0.000	0.566	0.640
Error	0.011	48	0.000		

The pH in the stream at MOSE remained fairly constant throughout the study ($F_{2,6}$ = 2.094, P = 0.270) between 7.52 ± 0.00 and 8.58 ± 0.07 (Figure 6.10). Interstitial pH was higher at the head of the bar than at the tail (P = 0.001, Table 6.6, Figure 6.10). At the tail of the bar, pH increased slightly as water was channelled over the bar (P = 0.033, Table 6.6, Figure 6.10).

6.4.3 Nitrogen dynamics

Surface total nitrogen at BOWM ranged from 0.395 ± 0.038 to 0.574 ± 0.053 mg/L during the study. Surface concentrations remained relatively constant among treatments ($F_{2,6}$ = 0.67, P = 0.575, Figure 6.11), but within-treatments, concentrations differed with each time ($F_{3,6}$ = 0.036, P = 0.002). Parafluvial TN was higher at 10 cm than at 30 cm (P = 0.002, Table 6.6, Figure 6.11), but displayed no increase or decrease consistent with the flow diversion (P = 0.787, Table 6.6, Figure 6.11). There was a negative correlation between interstitial TN and EC (r_{71} = -0.334, P = 0.046).

Stream TN concentrations at MOSE ranged between 0.105 ± 0.019 and 0.404 ± 0.017 mg/L. The concentration in the surface water was higher before and after the flow diversion ($F_{2,6}$ = 12.165, P = 0.036, Figure 6.11). Interstitial TN was highest in the head of the bar at 10 cm than at an any other location or depth (P = 0.005, Table 6.6, Figure 6.11). TN at MOSE correlated positively with DO (r_{71} = 0.490, P = 0.003) and negatively with EC (r_{71} = -0.496, P = 0.002).

Mean ammonium concentrations in the surface stream at BOWM ranged between 0.044 ± 0.010 and 0.056 ± 0.012 mg/L during this study and did not vary significantly with treatment ($F_{2,3}$ = 0.26, P = 0.784, Figure 6.12). Mean interstitial ammonium concentrations were higher in both habitats during the release, than before it (Figure 6.12), but massive variation among replicates rendered this difference non-significant (P = 0.301, Table 6.7). Interstitial concentrations remained relatively constant among times, lying between 0.032 ± 0.001 and 0.057 ± 0.014 mg/L. There was no change in ammonium concentration among habitats (P = 0.369, Table 6.7) or depths (P = 0.167, Table 6.7).

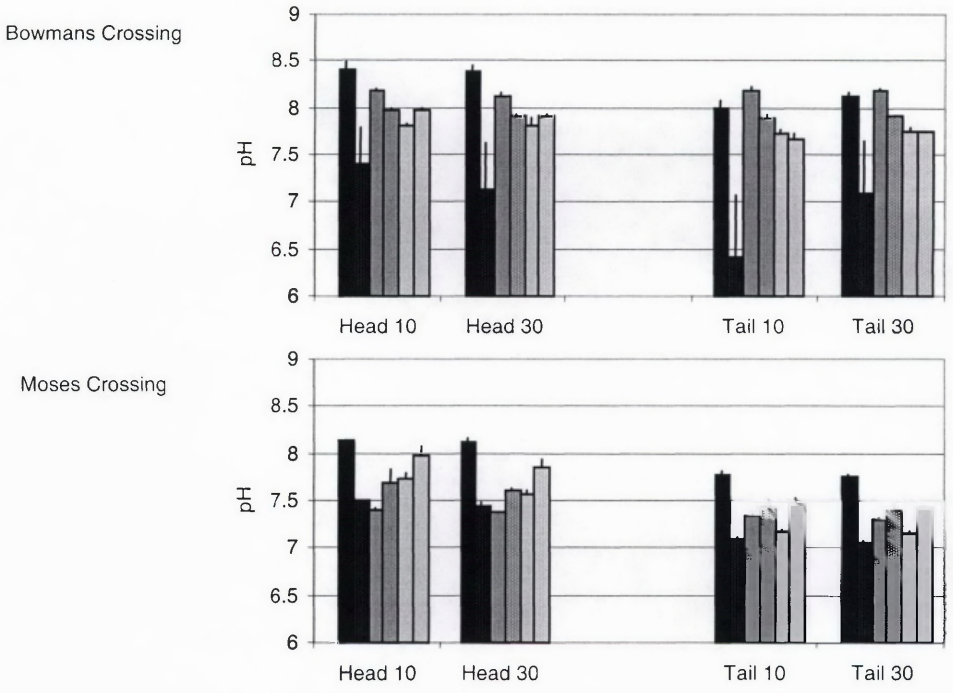

Surface pH	Time 1	Time 2	Time 3	Time 4	Time 5	Time 6
Bowmans Crossing	8.41 ± 0.14	8.25 ± 0.03	7.75 ± 0.06	8.38 ± 0.13	8.07 ± 0.00	8.76 ± 0.10
Moses Crossing	8.58 ± 0.07	7.57 ± 0.02	7.52 ± 0.00	7.93 ± 0.04	7.94 ± 0.11	7.76 ± 0.11

Figure 6.10. Mean (+ SE) pH at Bowmans Crossing and Moses Crossing over the six times of the survey. Table beneath graphs indicates mean (± SE) surface values.

Table 6.5. ANOVA results table for pH for the main factors and interaction terms. Bold figures are significant at P = 0.05. Tr = Treatment, H = Habitat, D = Depth, T(Tr) = Time nested in Treatment.

Source	SS	df	MS	F-ratio	P
Bowmans Crossing - rank transformed					
Tr	7057.771	2	3528.885	0.708	0.560
H	2266.889	1	2266.889	8.532	0.061
D	0.681	1	0.681	0.123	0.749
Tr*H	814.674	2	407.337	1.533	0.348
Tr*D	183.549	2	91.774	16.582	**0.024**
H*D	300.125	1	300.125	3.109	0.084
Tr*D*H	17.062	2	8.531	0.840	0.513
T(Tr)	14963.063	3	4987.688	51.675	**0.000**
H*T(Tr)	797.104	3	265.701	2.753	0.053
D*T(Tr)	16.604	3	5.535	0.057	0.982
H*D*T(Tr)	30.479	3	10.160	0.105	0.957
Error	4633.000	48	96.521		
Moses Crossing					
Tr	0.315	2	0.157	0.142	0.873
H	2.027	1	2.027	156.674	**0.001**
D	0.052	1	0.052	226.723	**0.001**
Tr*H	0.338	2	0.169	13.049	**0.033**
Tr*D	0.012	2	0.006	25.452	**0.013**
H*D	0.010	1	0.010	1.190	0.281
Tr*D*H	0.010	2	0.005	3.315	0.174
T(Tr)	3.330	3	1.110	134.822	**0.000**
H*T(Tr)	0.039	3	0.013	1.571	0.209
D*T(Tr)	0.001	3	0.000	0.028	0.994
H*D*T(Tr)	0.005	3	0.002	0.185	0.906
Error	0.395	48	0.008		

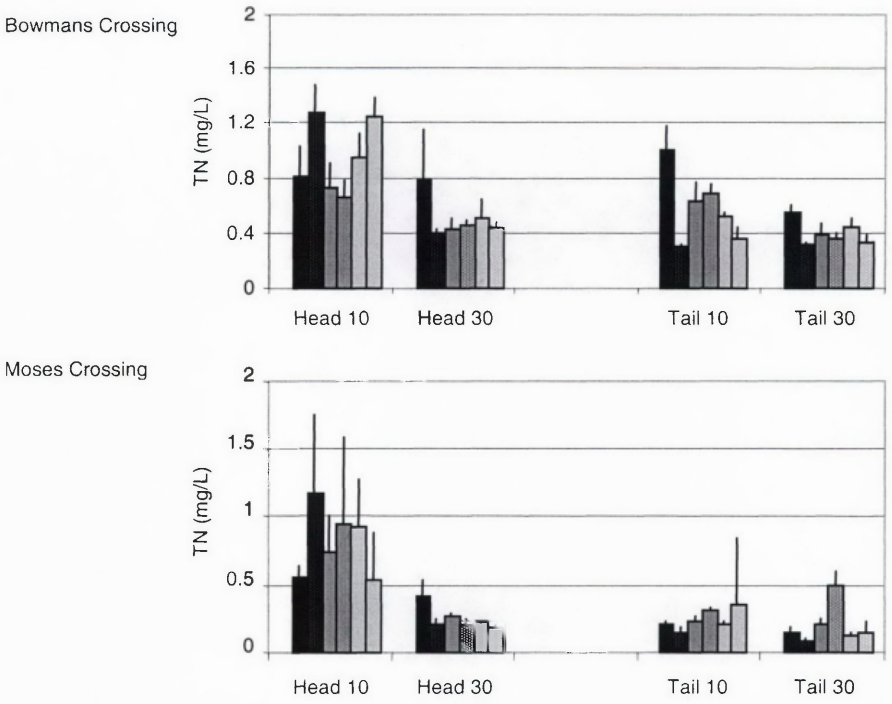

Surface TN (mg/L)	Time 1	Time 2	Time 3	Time 4	Time 5	Time 6
Bowmans Crossing	0.400 ± 0.023	0.413 ± 0.048	0.395 ± 0.038	0.574 ± 0.053	0.445 ± 0.012	0.432 ± 0.022
Moses Crossing	0.404 ± 0.017	0.274 ± 0.046	0.164 ± 0.004	0.207 ±0.009	0.400 ± 0.035	0.105 ± 0.019

Figure 6.11. Mean (+ SE) total nitrogen at Bowmans Crossing and Moses Crossing over the six times of the survey. Table beneath graphs indicates mean (± SE) surface values.

Table 6.6. ANOVA results table for total nitrogen for the main factors and interaction terms. Bold figures are significant at P = 0.05. Tr = Treatment, H = Habitat, D = Depth, T(Tr) = Time nested in Treatment.

Source	SS	df	MS	F-ratio	P
Bowmans Crossing - Log transformed					
Tr	0.039	2	0.019	0.260	0.787
H	0.443	1	0.443	4.972	0.112
D	0.774	1	0.774	110.889	**0.002**
Tr*H	0.117	2	0.058	0.656	0.581
Tr*D	0.001	2	0.000	0.045	0.957
H*D	0.076	1	0.076	4.222	**0.045**
Tr*D*H	0.098	2	0.049	0.687	0.568
T(Tr)	0.223	3	0.074	4.121	**0.011**
H*T(Tr)	0.268	3	0.089	4.942	**0.005**
D*T(Tr)	0.021	3	0.007	0.387	0.763
H*D*T(Tr)	0.215	3	0.072	3.967	**0.013**
Error	0.866	48	0.018		
Moses Crossing - Log(x + 1)					
Tr	0.010	2	0.005	1.946	0.287
H	0.119	1	0.119	20.691	**0.020**
D	0.101	1	0.101	21.460	**0.019**
Tr*H	0.016	2	0.008	1.387	0.375
Tr*D	0.002	2	0.001	0.238	0.802
H*D	0.071	1	0.071	8.604	**0.005**
Tr*D*H	0.005	2	0.002	0.303	0.759
T(Tr)	0.007	3	0.002	0.300	0.825
H*T(Tr)	0.017	3	0.006	0.698	0.558
D*T(Tr)	0.014	3	0.005	0.572	0.636
H*D*T(Tr)	0.022	3	0.007	0.906	0.445
Error	0.397	48	0.008		

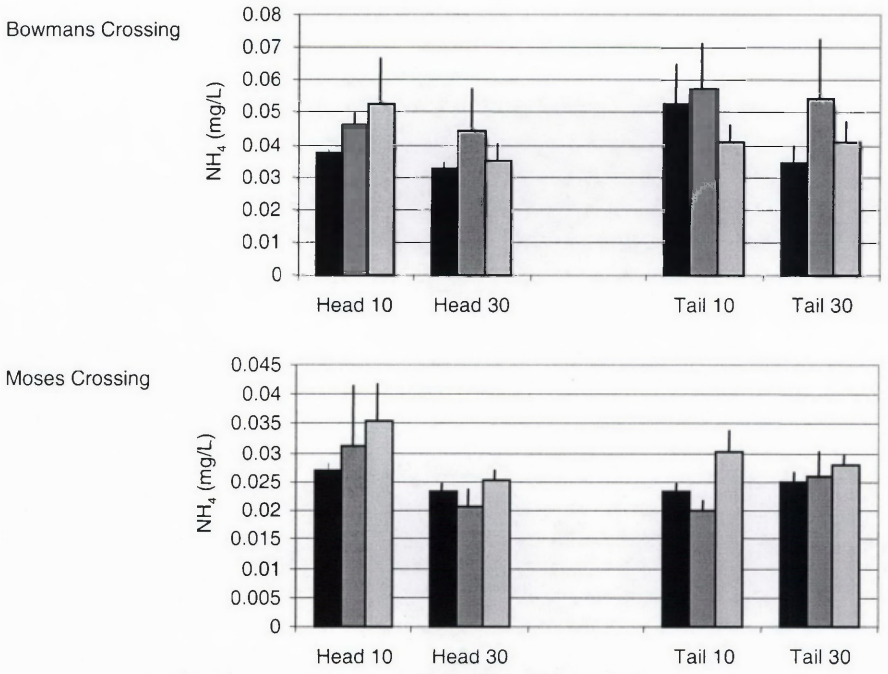

Surface NH_4 (mg/L)	Before	During	After
Bowmans Crossing	0.048 ± 0.007	0.044 ± 0.010	0.056 ±0.012
Moses Crossing	0.026 ± 0.000	0.029 ±0.000	0.035 ± 0.003

Figure 6.12. Mean (+ SE) ammonium at Bowmans Crossing and Moses Crossing over the six times of the survey. Table beneath graphs indicates mean (± SE) surface values.

Table 6.6. ANOVA results table for total nitrogen for the main factors and interaction terms. Bold figures are significant at P = 0.05. H = Habitat, D = Depth, T = Time.

Source	SS	df	MS	F-ratio	P
Bowmans Crossing - Square root transformed					
T	0.004	2	0.002	1.261	0.301
H	0.001	1	0.001	0.838	0.369
D	0.003	1	0.003	2.026	0.167
T*H	0.001	2	0.001	0.350	0.709
T*D	0.001	2	0.000	0.193	0.825
D*H	0.000	1	0.000	0.013	0.911
T*D*H	0.002	2	0.001	0.612	0.551
Error	0.036	24	0.001		
Moses Crossing - fourth root transformed					
T	0.003	2	0.002	2.901	0.074
H	0.000	1	0.000	0.386	0.540
D	0.001	1	0.001	1.612	0.216
T*H	0.000	2	0.000	0.033	0.967
T*D	0.000	2	0.000	0.442	0.648
D*H	0.003	1	0.003	4.897	**0.037**
T*D*H	0.001	2	0.000	0.571	0.573
Error	0.014	24	0.001		

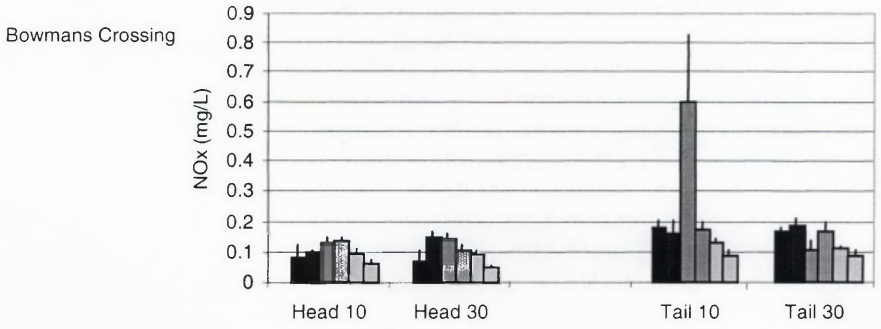

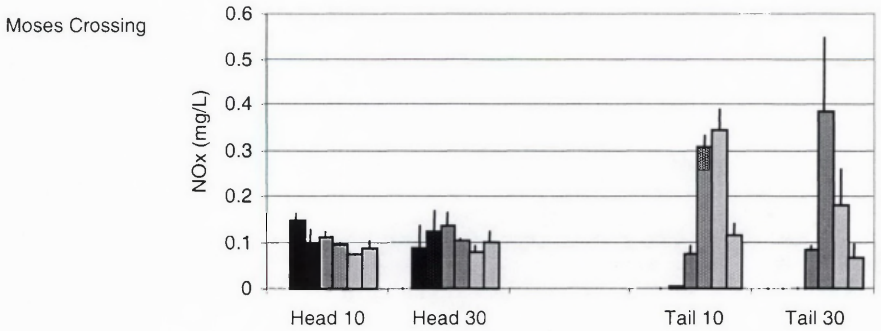

Surface NOx (mg/L)	Time 1	Time 2	Time 3	Time 4	Time 5	Time 6
Bowmans Crossing	0.011 ± 0.001	0.149 ± 0.003	0.103 ± 0.014	0.122 ± 0.004	0.132 ± 0.005	0.053 ± 0.001
Moses Crossing	0.049 ± 0.007	0.031 ± 0.007	0.082 ± 0.021	0.084 ± 0.023	0.106 ± 0.032	0.117 ± 0.025

Figure 6.13. Mean (+ SE) nitrate and nitrite nitrogen at Bowmans Crossing and Moses Crossing over the six times of the survey. Table beneath graphs indicates mean (± SE) surface values.

Table 6.8. ANOVA results table for nitrate and nitrite nitrogen for the main factors and interaction terms. Bold figures are significant at P = 0.05. Tr = Treatment, H = Habitat, D = Depth, T(Tr) = Time nested in Treatment.

Source	SS	df	MS	F-ratio	P
Bowmans Crossing - Log transformed					
Tr	0.845	2	0.422	2.675	0.215
H	0.841	1	0.841	11.016	**0.045**
D	0.056	1	0.056	1.419	0.319
Tr*H	0.120	2	0.060	0.785	0.532
Tr*D	0.168	2	0.084	2.126	0.266
H*D	0.067	1	0.067	1.818	0.184
Tr*D*H	0.078	2	0.039	0.473	0.663
T(Tr)	0.474	3	0.158	4.297	**0.009**
H*T(Tr)	0.229	3	0.076	2.078	0.115
D*T(Tr)	0.119	3	0.040	1.077	0.368
H*D*T(Tr)	0.246	3	0.082	2.233	0.096
Error	1.764	48	0.037		
Moses Crossing - square root transformed					
Tr	0.562	2	0.281	5.600	0.097
H	0.018	1	0.018	0.226	0.667
D	0.009	1	0.009	3.164	0.173
Tr*H	0.631	2	0.315	3.863	0.148
Tr*D	0.023	2	0.011	4.082	0.139
H*D	0.007	1	0.007	0.973	0.329
Tr*D*H	0.029	2	0.014	2.908	0.199
T(Tr)	0.151	3	0.050	7.367	**0.000**
H*T(Tr)	0.245	3	0.082	11.978	**0.000**
D*T(Tr)	0.008	3	0.003	0.404	0.750
H*D*T(Tr)	0.015	3	0.005	0.725	0.542
Error	0.327	48	0.007		

MOSE ammonium concentrations were unaffected by the flow manipulations in the surface ($F_{2,3} = 4.40$, $P = 0.128$) where concentrations ranged from 0.026 ± 0.001 and 0.035 ± 0.003 mg/L, and interstitially ($P = 0.074$, Table 6.7). Interstitial ammonium was highest (0.027 ± 0.001 to 0.036 ± 0.006 mg/L) at 10 cm at the head of the bar ($P = 0.037$, Table 6.7, Figure 6.12).

Mean NOx concentrations in the surface water at BOWM were higher during the flow diversion than at any of the other times ($F_{2,6} = 34.73$, $P = 0.008$, Figure 6.13). During the period of this study the lowest (0.011 ± 0.001 mg/L), and highest (0.149 ± 0.003 mg/L) concentrations occurred during the pre-diversion times. Interstitial NOx at BOWM was unaffected by the diversion, but was generally higher at the tail of the bar than at the head of the bar ($P = 0.045$, Figure 6.13, Table 6.8). At BOWM, interstitial NOx correlated with EC ($r_{71} = 0.382$, $P = 0.021$).

NOx in the surface water at MOSE did not vary significantly among treatments ($F_{2,6} = 7.09$, $P = 0.069$), ranging between 0.031 ± 0.007 mg/L during the second sampling, and 0.117 ± 0.025 mg/L at in the final sampling. Interstitial nitrate was higher (most concentrations over 0.3 mg/L) at Times 3 and 4, especially at the tail habitat ($P < 0.001$, Figure 6.13, Table 6.8). There was a negative relationship between NOx and pH ($r_{71} = -0.4062$, $P = 0.016$).

6.4.4 Phosphorus dynamics

Surface TP was high at BOWM immediately following the commencement of diversion (0.433 ± 0.296 mg/L) but otherwise remained constantly between 0.062 ± 0.001 mg/L and 0.086 ± 0.007 mg/L ($F_{2,6} = 0.63$, $P = 0.591$, Figure 6.14). Interstitial TP was higher at 10 cm depth than at 30 cm ($P = 0.008$, Table 6.9, Figure 6.14), especially at the head of the bar ($P = 0.003$, Table 6.9, Figure 6.14) but concentration was not affected by the diversion. TP at BOWM correlated with EC ($r_{71} = -0.360$, $P = 0.0312$).

Surface concentrations of TP were relatively constant at MOSE ($F_{2,6} = 0.443$, $P = 0.678$). Again interstitial TP was highest at 10 cm in than at 30 cm ($P = 0.003$, Table 6.9, Figure 6.14). TP was also higher at the head of the bar than the tail ($P = 0.013$, Table 6.9, Figure 6.14). There was a major drop in TP from Time 1 to Time 2 for all locations except at the head at 10 cm ($P = 0.002$, Table 6.9, Figure 6.14). The flow

diversion did not appear to affect subsurface TP at this site. TP correlated with DO (r_{71} = 0.413, P = 0.014) and pH (r_{71} = 0.586, P < 0.001).

In-stream SRP concentrations changed with treatment ($F_{2,3}$ = 32.57, P = 0.009) at BOWM, being lowest during the flow diversion (Figure 6.15). Throughout the study, surface concentrations ranged from 0.016 ± 0.001 to 0.080 ± 0.017 mg/L, being highest during Time 1 (Figure 6.15). Interstitial SRP was highest during the first sample occasion (P < 0.001, Table 6.10, Figure 6.15). At both depths at the two habitats, except the 10 cm depth at the head of the bar, SRP rose slightly following the release (Figure 6.15) but the high concentrations in the first pre-diversion time probably masked the significance of this. SRP concentrations corresponded negatively with EC (r_{71} = -0.615, P < 0.001).

During this study SRP in the surface water at MOSE did not change significantly as water was diverted over the bar ($F_{2,6}$ = 2.43, P = 0.236, Figure 6.15). Interstitial patterns were characterised by a decrease in SRP with the commencement of flow diversion, followed by an increase in concentration after the deflection fence was removed (P = 0.025, Table 6.10, Figure 6.15). At MOSE, the correlation between SRP and DO was negative (r_{71} = - 0.717, P < 0.001) but it was positive between SRP and EC (r_{71} = 0.404, P = 0.016).

6.4.5 Microbial hydrolytic activity

Hydrolytic activity at BOWM differed over time at each habitat and depth (P = 0.017, Table 6.11, Figure 6.16). At the head of the bar there was a decrease in activity at both depths during the flow diversion, but activity increased substantially afterward (Figure 6.16). Hydrolasic activity at 10 cm in the tail of the bar was also stimulated following the diversion, but this was not so for the deeper sediments (Figure 6.16).

The channelling of water over the bar at MOSE resulted in the opposite trend to that observed at BOWM; FDA increased in both habitats and depths except the deep sediments of the tail (P = 0.027, Table 6.11, Figure 6.16). Once flow was removed from the bar, FDA declined at 10 cm at both habitats, but increased at 30 cm (Figure 6.16).

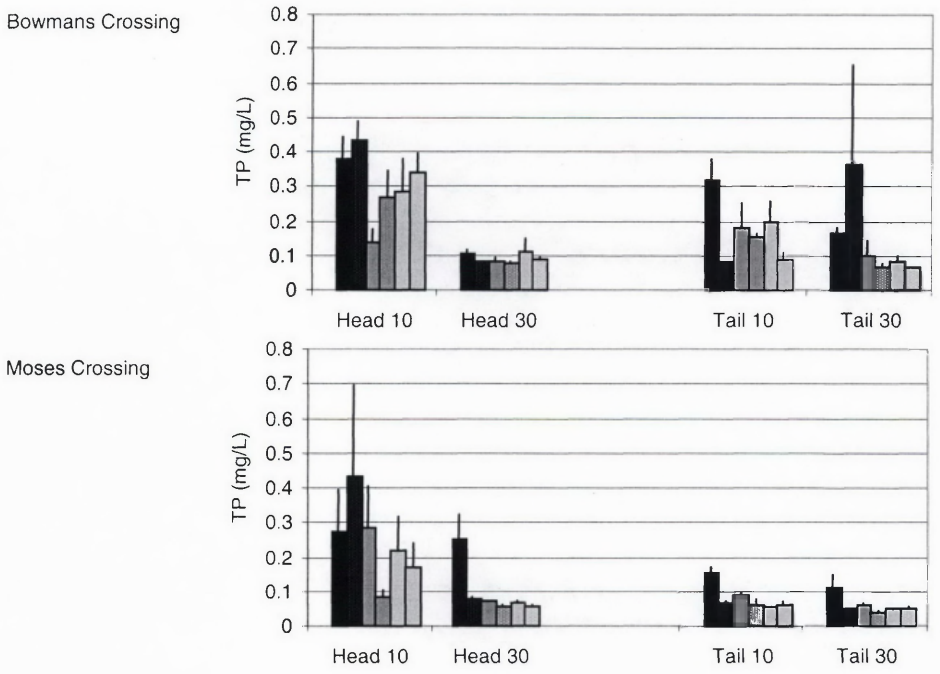

Surface TP (mg/L)	Time 1	Time 2	Time 3	Time 4	Time 5	Time 6
Bowmans Crossing	0.065 ± 0.005	0.086 ± 0.007	0.433 ± 0.296	0.075 ± 0.005	0.062 ± 0.000	0.076 ± 0.001
Moses Crossing	0.073 ± 0.001	0.051 ± 0.020	0.050 ± 0.009	0.053 ± 0.008	0.041 ± 0.003	0.059 ± 0.002

Figure 6.14. Mean (+ SE) total phosphorus at Bowmans Crossing and Moses Crossing over the six times of the survey. Table beneath graphs indicates mean (± SE) surface values.

Table 6.9. ANOVA results table for total phosphorus for the main factors and interaction terms. Bold figures are significant at P = 0.05. Tr = Treatment, H = Habitat, D = Depth, T(Tr) = Time nested in Treatment.

Source	SS	df	MS	F-ratio	P
Bowmans Crossing - Log transformed					
Tr	0.490	2	0.245	3.895	0.147
H	0.246	1	0.246	2.900	0.187
D	2.004	1	2.004	40.109	**0.008**
Tr*H	0.163	2	0.082	0.962	0.476
Tr*D	0.009	2	0.004	0.088	0.918
H*D	0.430	1	0.430	9.986	**0.003**
Tr*D*H	0.292	2	0.146	1.410	0.370
T(Tr)	0.189	3	0.063	1.459	0.238
H*T(Tr)	0.255	3	0.085	1.970	0.131
D*T(Tr)	0.150	3	0.050	1.159	0.335
H*D*T(Tr)	0.311	3	0.104	2.403	0.079
Error	2.069	48	0.043		
Moses Crossing - rank transformed					
Tr	3187.646	2	1593.823	0.981	0.470
H	4309.014	1	4309.014	28.535	**0.013**
D	3901.389	1	3901.389	76.613	**0.003**
Tr*H	101.549	2	50.774	0.336	0.738
Tr*D	287.174	2	143.587	2.820	0.205
H*D	120.125	1	120.125	0.437	0.512
Tr*D*H	469.521	2	234.760	22.522	**0.016**
T(Tr)	4875.021	3	1625.007	5.908	**0.002**
H*T(Tr)	453.021	3	151.007	0.549	0.651
D*T(Tr)	152.771	3	50.924	0.185	0.906
H*D*T(Tr)	31.271	3	10.424	0.038	0.990
Error	13203.000	48	275.063		

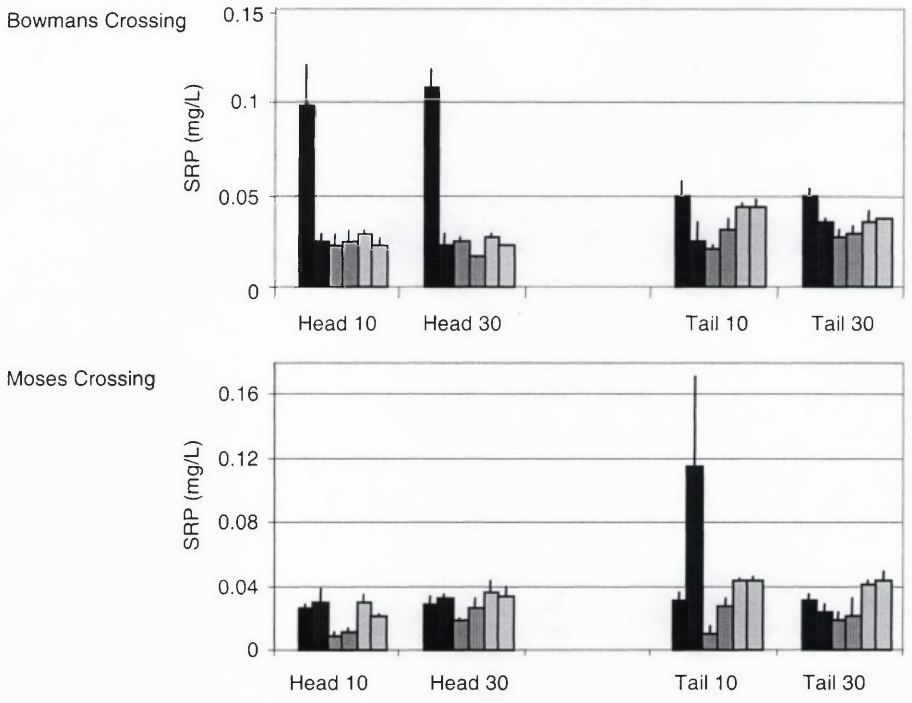

Surface SRP (mg/L)	Time 1	Time 2	Time 3	Time 4	Time 5	Time 6
Bowmans Crossing	0.080 ± 0.017	0.026 ± 0.003	0.016 ± 0.001	0.018 ± 0.000	0.030 ± 0.004	0.021 ± 0.000
Moses Crossing	0.027 ± 0.014	0.029 ± 0.009	0.002 ± 0.001	0.010 ± 0.001	0.028 ± 0.003	0.029 ± 0.002

Figure 6.15. Mean (+ SE) soluble reactive phosphorus at Bowmans Crossing and Moses Crossing over the six times of the survey. Table beneath graphs indicates mean surface values.

Table 6.10. ANOVA results table for soluble reactive phosphorus for the main factors and interaction terms. Bold figures are significant at P = 0.05. Tr = Treatment, H = Habitat, D = Depth, T(Tr) = Time nested in Treatment.

Source	SS	df	MS	F-ratio	P
Bowmans Crossing - Log transformed					
Tr	0.807	2	0.404	1.014	0.461
H	0.046	1	0.046	0.456	0.548
D	0.000	1	0.000	0.005	0.950
Tr*H	0.292	2	0.146	1.439	0.365
Tr*D	0.027	2	0.013	1.098	0.439
H*D	0.011	1	0.011	0.774	0.383
Tr*D*H	0.034	2	0.017	1.470	0.359
T(Tr)	1.194	3	0.398	28.219	**0.000**
H*T(Tr)	0.304	3	0.101	7.195	**0.000**
D*T(Tr)	0.036	3	0.012	0.862	0.467
H*D*T(Tr)	0.034	3	0.011	0.812	0.493
Error	0.677	48	0.014		
Moses Crossing - rank transformed					
Tr	12388.563	2	6194.281	16.146	**0.025**
H	1730.681	1	1730.681	11.939	**0.041**
D	369.014	1	369.014	4.016	0.139
Tr*H	1511.299	2	755.649	5.213	0.106
Tr*D	486.715	2	243.358	2.649	0.217
H*D	1317.556	1	1317.556	5.918	**0.019**
Tr*D*H	37.674	2	18.837	0.081	0.924
T(Tr)	1150.896	3	383.632	1.723	0.175
H*T(Tr)	434.896	3	144.965	0.651	0.586
D*T(Tr)	275.646	3	91.882	0.413	0.745
H*D*T(Tr)	698.396	3	232.799	1.046	0.381
Error	10687.167	48	222.649		

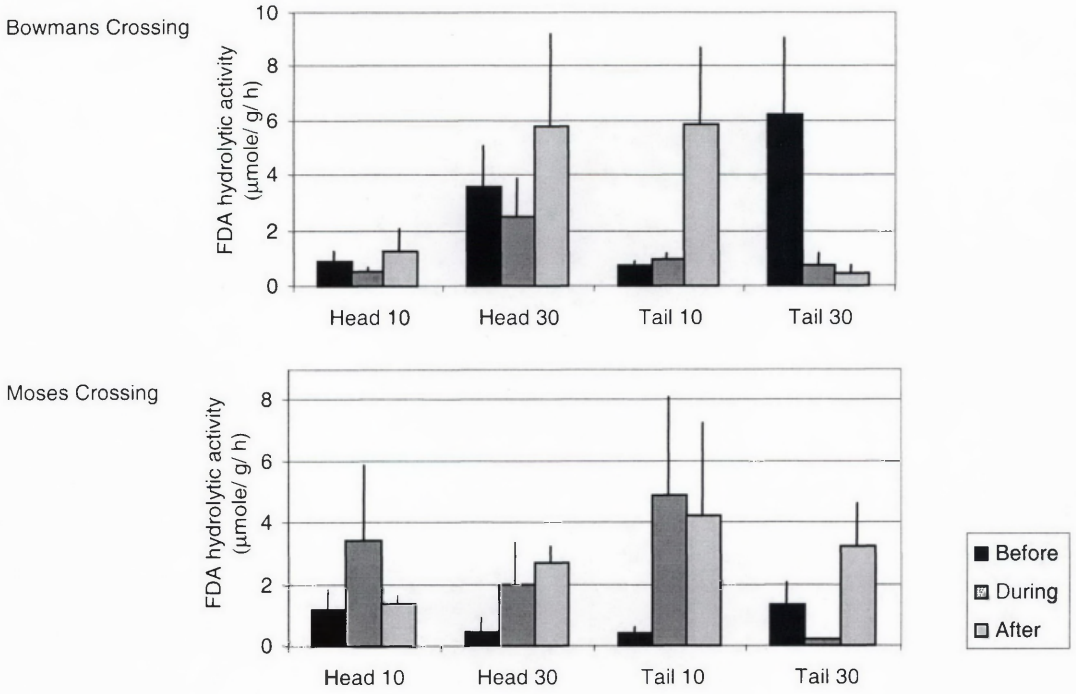

Figure 6.16. Mean (+ SE) bacterial hydrolytic activity at Bowmans Crossing and Moses Crossing.

Table 6.11. ANOVA results table for bacterial hydrolytic activity for the main factors and interaction terms. Bold figures are significant at P = 0.05. H = Habitat, D = Depth, T = Time.

Source	SS	df	MS	F-ratio	P
Bowmans Crossing - Log(x+1) transformed					
T	0.280	2	0.140	2.418	0.110
H	0.007	1	0.007	0.112	0.740
D	0.216	1	0.216	3.728	0.065
T*H	0.048	2	0.024	0.416	0.664
T*D	0.440	2	0.220	3.795	**0.037**
D*H	0.338	1	0.338	5.833	**0.024**
T*D*H	0.564	2	0.282	4.867	**0.017**
Error	1.390	24	0.058		
Moses Crossing - Fourth root transformed					
T	1.292	2	0.646	4.259	**0.027**
H	0.000	4	0.000	0.002	0.965
D	0.106	4	0.106	0.700	0.412
T*H	0.145	2	0.073	0.480	0.625
T*D	0.353	2	0.177	1.165	0.330
D*H	0.029	1	0.029	0.189	0.668
T*D*H	0.302	2	0.151	0.995	0.385
Error	3.487	23	0.152		

6.4.6 Faunal dynamics

At BOWM there were more invertebrates in the head of the bar at 10 cm ($P = 0.001$, Table 6.12) than at other habitats and depths (Figure 6.17). There was a decrease in invertebrate abundance while water was flowing over the bar ($P = 0.003$, Table 6.12, Figure 6.17). Taxonomic richness was highest at the head of the BOWM bar ($P = 0.044$, Table 6.13, Figure 6.18) and did not change with time.

More invertebrates were present in the head of the bar at MOSE than at the tail ($P < 0.001$, Table 6.12, Figure 6.17), and there were more at 10 cm than 30 cm ($P = 0.034$, Table 6.12, Figure 6.17). More taxa inhabited the shallow tail of the MOSE bar than any other depth and habitat ($P = 0.012$, Table 6.13, Figure 6.18). Taxonomic richness correllated with DO ($r_{35} = 0.337$, $P = 0.048$).

Community analysis at BOWM showed that the composition of fauna changed with time (Global $R = 0.189$, $P = 0.003$, Figure 6.19). While communities during and after the diversion were similar to each other (pairwise $R = -0.113$, $P = 0.923$), dominated by oligochaetes, cyclopoids, chironomids, and leptophlebiid mayflies, they were both different to the pre-diversion fauna (R before - during = 0.389; R before – after = 0.290, both $P < 0.001$). The pre-diversion fauna was dominated by oligochaetes, microturbellarians, and cyclopoids. Communities at BOWM differed among habitats (Global $R = 0.175$, $P = 0.011$, Figure 6.19), with chironomids being common at the head of the bar, and microturbellarians common at the tail. Both depths had a similar fauna (Global $R = 0.047$, $P = 0.241$) dominated by oligochaetes, cyclopoids, and microturbellatians.

The MOSE community structure was not affected by the release (Global $R = 0.089$, $P = 0.061$, Figure 6.20), and at all times microturbellarians and oligochaetes dominated the fauna. Invertebrate community composition was associated with location in the bar (Global $R = 0.467$, $P < 0.001$, Figure 6.20) with the head of the bar having five dominant taxa (oligochaetes, microturbellarians, nematodes, *Wandesia* sp. mites, and cyclopoids) and the tail having only two taxa (microturbellarians and oligochaetes). Both deep and shallow sediments were dominated by microturbellarians and oligochaetes (Global $R = 0.059$, $P = 0.166$).

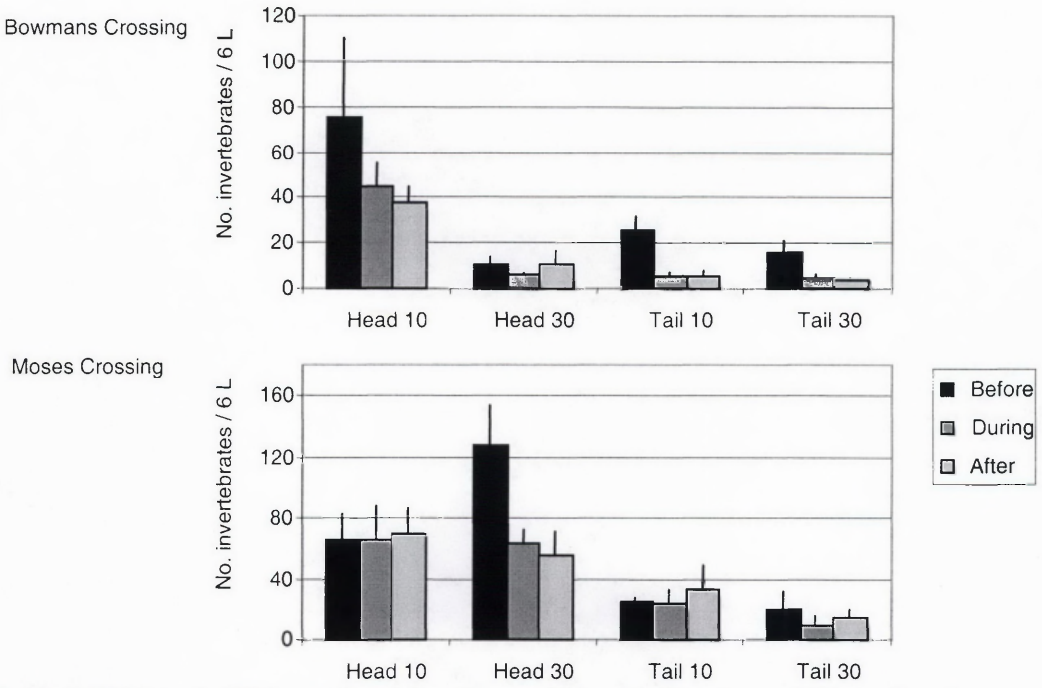

Figure 6.17. Mean (+ SE) invertebrate abundance at Bowmans Crossing and Moses Crossing.

Table 6.12. ANOVA results table for invertebrate abundance for the main factors and interaction terms. Bold figures are significant at P = 0.05. H = Habitat, D = Depth, T = Time.

Source	SS	df	MS	F-ratio	P
Bowmans Crossing - Log(x+1) transformed					
T	0.966	2	0.483	7.660	**0.003**
H	1.267	1	1.267	20.096	**0.000**
D	1.446	1	1.446	22.939	**0.000**
T*H	0.281	2	0.140	2.226	0.131
T*D	0.048	2	0.024	0.382	0.687
D*H	0.970	1	0.970	15.382	**0.001**
T*D*H	0.046	2	0.023	0.368	0.696
Error	1.450	23	0.063		
Moses Crossing - Log(x+1) transformed					
T	0.000	2	0.000	0.005	0.995
H	0.910	1	0.910	35.254	**0.000**
D	0.131	1	0.131	5.083	**0.034**
T*H	0.013	2	0.007	0.257	0.775
T*D	0.068	2	0.034	1.309	0.289
D*H	0.010	1	0.010	0.403	0.531
T*D*H	0.105	2	0.053	2.037	0.152
Error	0.619	24	0.026		

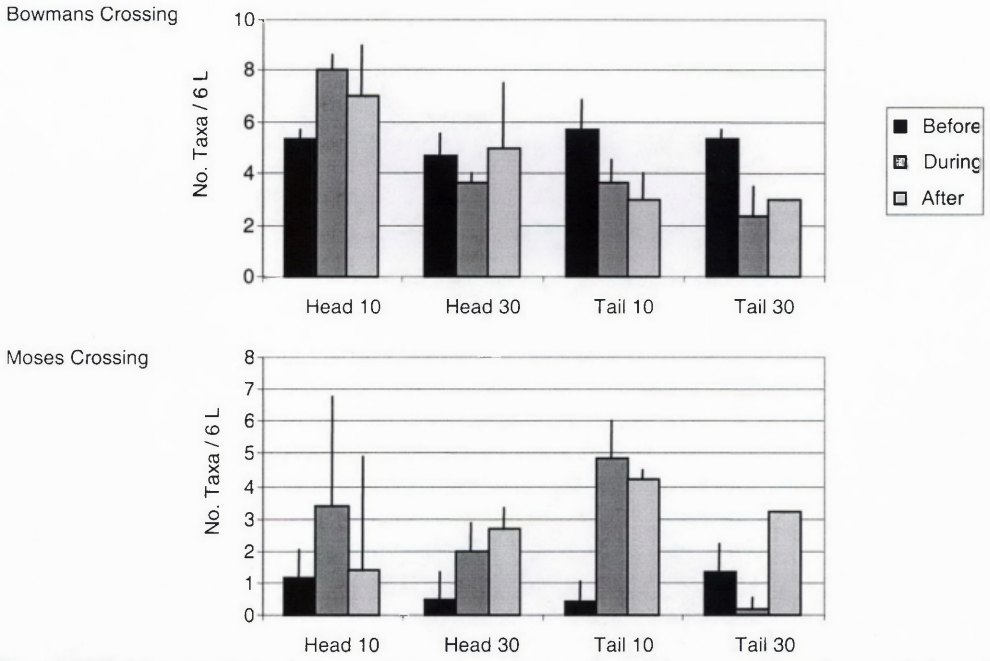

Figure 6.18. Mean (+ SE) numbers of taxa for each sample at Bowmans Crossing and Moses Crossing.

Table 6.13. ANOVA results table for taxa numbers for the main factors and interaction terms. Bold Figures are significant at P = 0.05. H = Habitat, D = Depth, T = Time.

Source	SS	df	MS	F-ratio	P
Bowmans Crossing - Log(x+1) transformed					
T	0.064	2	0.032	1.398	0.267
H	0.103	1	0.103	4.520	**0.044**
D	0.055	1	0.055	2.434	0.132
T*H	0.095	2	0.047	2.081	0.148
T*D	0.018	2	0.009	0.392	0.680
D*H	0.067	1	0.067	2.964	0.099
T*D*H	0.020	2	0.010	0.447	0.645
Error	0.523	23	0.023		
Moses Crossing - Log(x+1) transformed					
T	0.160	2	0.080	1.269	0.299
H	3.145	1	3.145	49.979	**0.000**
D	0.193	1	0.193	3.065	0.093
T*H	0.055	2	0.027	0.436	0.651
T*D	0.064	2	0.032	0.512	0.605
D*H	0.461	1	0.461	7.333	**0.012**
T*D*H	0.067	2	0.034	0.536	0.592
Error	1.510	24	0.063		

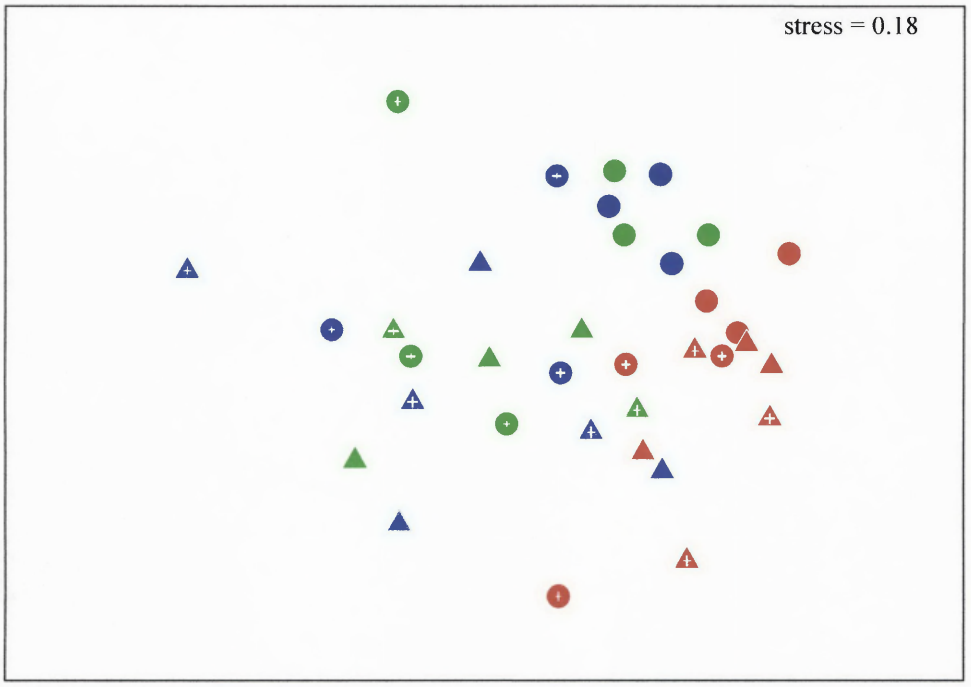

Figure 6.19. Non-metric multidimensional scaling plot for faunal communities at Bowmans Crossing. Red = 'before' samples, green = 'during' samples, blue = 'post' samples. Circle = downwelling, triangle = upwelling. Filled shapes = 10 cm, crossed shapes = 30 cm.

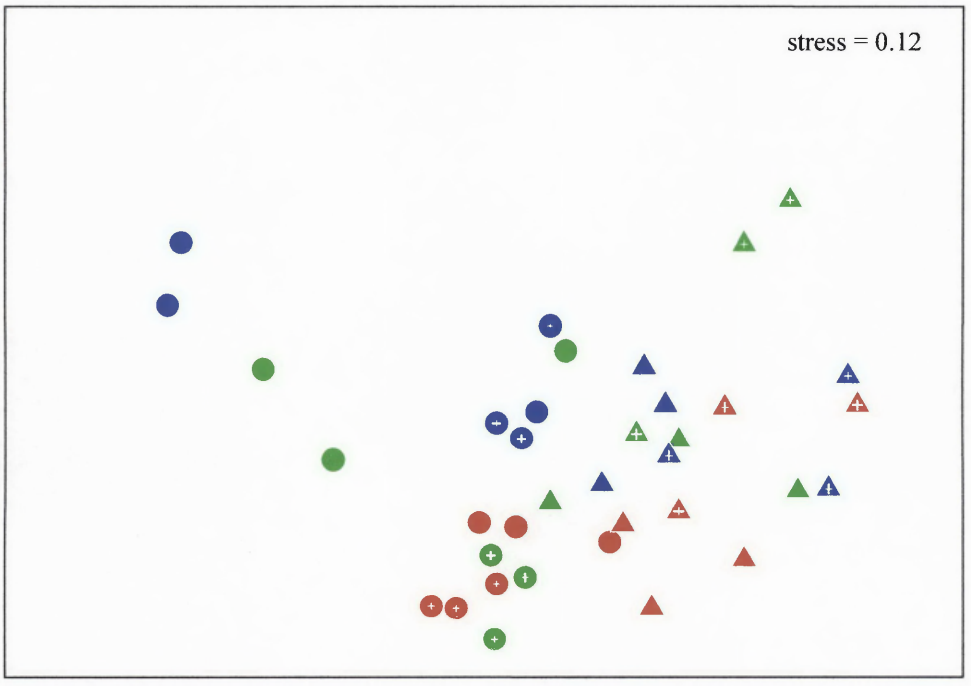

Figure 6.20. Non-metric multidimensional scaling plot for faunal communities at Moses Crossing. Red = 'before' samples, green = 'during' samples, blue = 'post' samples. Circle = downwelling, triangle = upwelling. Filled shapes = 10 cm, crossed shapes = 30 cm.

6.5 Discussion

Vertical hydraulic gradient

The diversion of water over the bar temporarily increased hydraulic exchange between the stream and the hyporheic zone at both sites. Increased downwelling and upwelling was expected as water rushed in to fill pore-spaces that were once filled by air. However, at BOWM there was no significant increase in downwelling, whereas upwelling increased. This is probably because downwelling occurred over a larger area than upwelling. At MOSE, the increased hydraulic head did not persist for the duration of the elevated flows, and it appears that a degree of equilibrium in exchange was reached.

Since, in all cases except the 10 cm tail at BOWM, the VHG returned to pre-diversion levels, it is unlikely that the small fluctuation reported here caused any significant flushing of fine particles as occurred in Chapter 5. Rather, the main cause for increased VHG during this study appeared to be hydraulic. The increase in hydraulic head that occurred with rising river stage emphasises the role of flow fluctuations in maintaining hydraulic links with the hyporheic zone (Hancock 2002).

In this study, hydraulic head at downwelling zones was always greater than it was at upwelling zones. Pepin and Hauer (2002) found similar patterns between the downwelling and upwelling zones of two steams in northwestern Montana, which attributed to downwelling zones being more concentrated in a spatial extent than the upwelling zones. Interstitial water does not travel in a straight line. Rather, it moves laterally or vertically through pore spaces (Wagner and Bretschko 2002). In the process, the water spreads out, resulting in dispersed upwelling zones. This is likely to be the case for the two sites in the Hunter River, since downwelling occurred in a spatially restricted area of about 4 m^2 immediately upstream of the bar, while the area of upwelling was probably more than 100 m^2.

Physico-chemical patterns

There has been some previous research supporting the argument that a temporary increase in surface stream flow causes increased dissolved oxygen in the hyporheic zone (Stanley and Boulton 1995, Chapter 5). Even a small rise in water level of less than 14 cm was enough to increase the dissolved oxygen at a hyporheic depth of 30 cm

in the Hunter River. The increased hydraulic head resulting from the rise in water level contributed to the higher interstitial dissolved oxygen, since there was a more rapid exchange here with the surface environment. Also, water travelling through the sediments during the flow deflection probably had a shorter residence time than before the release, with new, oxygen-rich water replacing water in which the oxygen was depleted.

Temperature fluctuations followed diel patterns, with morning temperatures being lower than evening temperatures. Diel patterns in temperature were also observed in three bars of Sycamore Creek, but temperature at the end of the bar appeared more buffered than those nearer the stream (Stanley and Boulton 1995). Valett (1993) also found the interstitial water temperature of Sycamore Creek to be buffered and to display longitudinal patterns with temperature that declined along subsurface flowpaths. The reason there was no temperature lag in the bars at BOWM and MOSE is because only short sections of each bar were sampled.

Electrical conductivity of hyporheic water at the head of the bar was not influenced by the release, but there was a drop in the conductivity at the tail of the bar at MOSE during the release. Interstitial water at the head of the bar was already largely influenced by surface water, so was affected little by the increase in downwelling water at the commencement of the diversion. However, before the release, the end of the bar was relatively isolated from the stream, water here moved slowly, and free ions possibly accumulated in the water. With inundation, the distance between the influent stream water and the tail of the bar was effectively shortened.

Nutrient patterns

Rises in stream water level have been found to increase the concentration of some forms of interstitial nitrogen (e.g. nitrite and nitrate nitrogen – Stanley and Boulton 1995, Martí *et al.* 1997, Chapter 5). However, the small increase in flow reported in this chapter had no impact on interstitial nitrogen concentration, either as total nitrogen, NOx nitrogen, or ammonium.

One effect of this flow diversion was hypothesised to be an increase in the concentration of NOx. However, despite increases in interstitial oxygen, which can stimulate bacterial nitrification (Mulholland *et al.* 1997), the diversion did not affect

NOx concentrations. There are two possible reasons for this. First, coupled with the increased VHG is an increase in the hydraulic conductivity of the sediments. This means that water flows faster through the sediments, removing NOx as it is formed and not allowing it to accumulate in higher concentrations. A second explanation for the lack of increased NOx could be slow interstitial bacterial activity. If bacterial activity is slow, or bacteria are present in low numbers, 12 h may not be long enough for interstitial NOx concentrations to increase significantly. Most likely, there is a combination of these two factors contributing to NOx concentrations being unchanged. Low numbers of nitrifying bacteria transform nitrogen to NOx, and it is then moved out of the sediments, rather than accumulating. If this was the case, then there would be higher concentrations of NOx in the tail of the bar, than in the head, which is the pattern observed at both sites.

Another of the effects predicted by the model was an increase in ammonium brought about by its liberation from sediments upon re-wetting, as was found in lake sediments by McComb and Qiu (1998). However, this did not eventuate at both of the Hunter River sites, with ammonium concentrations in the parafluvial sediments of the MOSE remaining unchanged. The reasons for this may be similar to those for the lack of significant increase in NOx: ammonium was released at a rate similar to that at which it was being removed (either by flushing or oxidation to NOx).

Interstitial concentrations of total phosphorus were highest in the shallow sediments at the head of the bar. The rise in water level had no observable impact on total phosphorus concentration. On the other hand, SRP at MOSE decreased in concentration as it was flushed from the sediments during the deflection. SRP increased again after the deflection fence was removed. BOWM SRP responded in a manner similar to this, but to a much lesser degree. These patterns contrast with the expectations of the model, where SRP was predicted to first increase with the diversion, then decrease after the resumption of normal flow. It is possible that there was some degree of phosphorus liberation from the sediments upon re-wetting (similar to the release from lake sediments – Qiu and McComb 1995) but that the increased interstitial flow rate prevented it from accumulating. When the diversion was removed, flow slowed and the accumulated SRP became evident.

A second explanation may be that a longer time period was needed to observe this effect. SRP accumulates in the sediments at BOWM more rapidly than at MOSE. As the sediments dry further, it is possible that bacteria will remove soluble phosphorus and incorporate it into particulate matter, as sometimes occurs in wetland sediments (McComb and Qiu (1998), but this was not captured in the time frame of this experiment.

Bacterial hydrolytic activity

The increase in hydrolytic activity during the flow deflection at MOSE support the hypothesis that hydrolytic activity is enhanced by greater downwelling. However, the patterns observed at BOWM do not. Generally, the strength of downwelling was always higher at MOSE than at BOWM, and MOSE FDA measurements were also higher overall. Of two sites in the Danube River, the one with the highest inflow of water had more hydrolytic activity than the other site (Battin and Sengschmitt 1999). Hydrolytic activity at a site on the Oberer Seebach, Austria, also increased with upwelling and downwelling velocities (Battin 2000). Nevertheless, both BOWM and MOSE experienced increased downwelling with the commencement of the diversion, so it is not clear why hydrolytic activity at MOSE increased while at BOWM it decreased. Hydrolytic activity at BOWM did increase after the deflection, so perhaps at this site the bacterial reaction was delayed.

Faunal community

This small increase in flow did not cause any significant change in the community structure at MOSE, where oligochaetes and microturbellarians dominated. In contrast to this, the BOWM faunal community behaved as expected with an influx of epigean taxa such as chironomid midge larvae and leptophlebiid mayfly nymphs. Perhaps the reason for this was due to the structure of the inundated area. At BOWM the area that was covered by the diversion was effectively an extension of the riffle edge, which would have been easily colonised by epigean fauna as water level increased. The area immediately upstream of the bar at MOSE was a small, still backwater, and the bar itself was more isolated from the main flow of the river than was the bar at BOWM. Since the increase in river height was only localised and small, there would not have been much invertebrate drift coming down the river, and more than likely, movement into the sediments would have been active. Therefore, to colonise the MOSE bar, epigean fauna had further to travel than they did for the BOWM bar. These

observations lend further support to the hyporheic refugia theory (Grimm *et al.* 1991). Small numbers of some epigean fauna (Ceratopogonidae, Empididae) did start to appear in the shallow sediments during and after the deflection, but not in high enough numbers to affect community structure. This may, in part, explain why there is an increase in richness at MOSE, despite there being a concurrent decline in invertebrate abundance, and no significant change in the community structure.

6.6 Conclusions

A small increase in water level for a period of 12 h failed to bring about the significant increases in nitrogen and phosphorus predicted by the model. Despite an increase in the vertical hydraulic gradient, and dissolved oxygen concentration, NOx was unaffected. While there may have been slight increases in NOx, it was probably prevented from increasing in concentration by the higher through-flow of water. This also applies to ammonium. SRP was affected by the flow diversion, first decreasing as water flushed it from the sediments, then increasing following the removal of the deflection fence. Nutrient concentrations may have been affected more if the period of inundation was longer than 12 h, or the magnitude of the flow was greater.

Increased hydraulic exchange and higher oxygen also contributed to increased bacterial hydrolytic activity, which was higher overall at MOSE, and increased at this site as water flowed over the bar as a consequence of more rapid exchange through the sediments. Hydrolytic activity at BOWM did not increase with water level, but appeared to have a lagged response.

Epigean invertebrate taxa became more common with increased flow at BOWM, but this was not the case at MOSE. With only a small increase in hydraulic pressure, it was concluded that invertebrate movement into the sediments was active rather than passive. In real flow situations, such as those resulting from Flow Rule 2, the small changes observed in this study are likely to be magnified, since the small 12-h flow increase is likely to occur concurrently with a longer term, larger flow.